Atmospheric Environment 382 (2026) 122220

Contents lists available at ScienceDirect

Atmospheric Environment

journal homepage: www.elsevier.com/locate/atmosenv

Review article

A systematic review of two LIF-based instruments for bioaerosol monitoring: Data treatment, performance evaluation, applications and comparison of WIBS and Rapid-E

Alessio Carminati [a,*], Andrea Spinazzè [a], Francesca Borghi [a,b], Stefano Boscolo [a], Giacomo Fanti [c], Eleonora Pagani [a], Carolina Zellino [a], Andrea Cattaneo [a], Domenico Maria Cavallo [a]

[a] Department of Science and High Technology, University of Insubria, Como, Italy
[b] Department of Medical and Surgical Sciences, University of Bologna, Bologna, Italy
[c] Department of Clinical Sciences and Community Health, University of Milan, Milan, Italy

HIGHLIGHTS

- WIBS and Rapid-E show size-dependent differences in particle counting.
- ML and clustering approaches improve UV-LIF bioaerosol classification.
- Indoor bioaerosols follow occupancy; weather drives outdoor levels.
- UV-LIF data show good correlations with traditional off-line methods.
- Standardized data protocols are needed to resolve study disparities.

ARTICLE INFO

Keywords:
Bioaerosols
UV-LIF
Wideband integrated bioaerosol sensor
WIBS
Rapid-E
Real-time bioaerosol monitoring

ABSTRACT

Biological aerosols are ubiquitous and can affect human health and atmospheric processes. Conventional off-line techniques, including culture-based methods, microscopy, and molecular approaches (e.g., PCR/NGS) provide information but are slow and unsuitable for capturing short-term dynamics. Ultraviolet light-induced fluorescence (UV-LIF) instruments enable real-time monitoring of bioaerosol, yet biological attribution remains challenging due to fluorescent interferents (such as PAHs, soot, mineral dust, and biomass-burning particles) and heterogeneous data treatment. This systematic review assesses the state-of-knowledge of two UV-LIF instruments, the Wideband Integrated Bioaerosol Sensor (WIBS) and Rapid-E(+), focusing on monitoring performance, data processing, application in outdoor and indoor environments, and comparison against other methods for the bioaerosols measurements. A literature search was performed on Scopus, Web of Science and PubMed using a search string. A total of 76 original articles were included (60 using WIBS, 13 using Rapid-E(+), 3 using both instruments). Outdoor field deployments dominate (n = 51), followed by laboratory studies (n = 32), whereas indoor campaigns remain scarce (n = 7); 20 studies included comparisons with other approaches for bioaerosol detection. Despite some discrepancies in counting performance of particles, with WIBS more reliably detecting finer particles (especially 1–2 μm) and Rapid-E(+) performing better for larger particles (i.e. > 10 μm), laboratory evidence shows a good ability to discriminate between biological and non-biological particles. The review further provides a structured synthesis of data-treatment approaches, validation needs and practical applicability across laboratory, indoor, outdoor and source-oriented settings. From indoor studies, the role of human occupancy and activities emerged, while in outdoor environments the presence of natural sources of

* Corresponding author.
E-mail addresses: acarminati@uninsubria.it (A. Carminati), andrea.spinazze@uninsubria.it (A. Spinazzè), francesca.borghi12@unibo.it (F. Borghi), sboscolo@studenti.uninsubria.it (S. Boscolo), giacomo.fanti@unimi.it (G. Fanti), epagani4@uninsubria.it (E. Pagani), czellino@uninsubria.it (C. Zellino), andrea.cattaneo@uninsubria.it (A. Cattaneo), domenico.cavallo@uninsubria.it (D.M. Cavallo).

https://doi.org/10.1016/j.atmosenv.2026.122220
Received 16 March 2026; Received in revised form 29 June 2026; Accepted 9 July 2026
Available online 11 July 2026

bioaerosol, meteorological and seasonal-related patterns, and the influence of anthropogenic interferents was evident.

Abbreviations

2D	two-dimensional
3D	three-dimensional
AF	Asphericity Factor
ANN	Artificial Neural Network
CCN/ICN	Cloud/Ice Condensation Nuclei
CFU	Colony Forming Units
CNN	Convolutional Neural Network
CPC	Condensation Particle Counter
dPCR	digital Polymerase Chain Reaction
DBSCAN	Density Based Spectral Clustering and Noise
dN/dlogAF	Asymmetry factor Distribution
DNA	Deoxyribonucleic Acid
EOD	Equivalent Optical Diameter
FAP	Fluorescent Aerosol Particle
FL	WIBS Fluorescence detection channel
HACA	Hierarchical Agglomerative Cluster Analysis
HULIS	Humic-like substances
HVAC	Heat Ventilation Air Conditioning
MC	Microbial Cultivation
ML	Machine Learning
MLP	Multilayer Perceptron
MVD	Median Volume Diameter
NADH	Nicotinamide Adenine Dinucleotide
NADPH	Nicotinamide Adenine Dinucleotide Phosphate
NGS	Next-Generation Sequencing
nm	nanometres
NO2	Nitorgen Dioxide
NOx	Nitrogen Oxides
OM	Optical Microscope
OMC	Optical Microscopy Counting
OPC	Optical Particle Counter
PAH	Polycyclic Aromatic Hydrocarbons
PBAPs	Primary Biological Aerosol Particles
PCR	Polymerase Chain Reaction
PDF	Probability Density Function
PSL	Polystyrene Latex
qPCR	quantitative Polymerase Chain Reaction
RH	Relative Humidity
RMSD	Root Mean Square Error Deviation
RNA	Ribonucleic Acid
SAS	Surface Air System
SOA	Secondary Organic Aerosols
UV-LIF	Ultraviolet-Laser-Induced-Fluorescence
WIBS	Wideband Integrated Bioaerosol Sensor
WSOD	Weakly Supervised Object Detection

1. Introduction

1.1. Bioaerosol: general overview

Biological aerosols (or “bioaerosols”, also referred to as “Primary Biological Aerosol Particles – PBAPs”) are a subset of ubiquitous indoor and outdoor airborne particles of biological origin, varying in size and shape. These include viruses (0.01-0.3 μm), bacteria (0.5-5 μm) and their agglomerates (up to 10 μm), fungal spores (0.5-30 μm), pollens (5-100 μm), and also fragments or excretions (e.g., animal and plant debris, metabolic by-products, etc.) (Cheng et al., 2020; Crawford et al., 2014; Forde et al., 2019a; Zhang and Lai, 2025). Bioaerosols are of particular concern because they can influence environmental processes, acting as Cloud or Ice Condensation Nuclei (CCN or ICN) and thereby affecting the radiative balance, cloud formation and precipitation. They can also affect living organisms, including humans since they can be inhaled, potentially reaching the lung's alveolar region, and cause or exacerbate numerous respiratory illnesses (e.g., asthma and chronic obstructive pulmonary disease), infections, allergies, cardiovascular diseases and cancer (Addor et al., 2022; Calvo et al., 2018; Forde et al., 2019a; Morrison et al., 2020; O'Connor et al., 2013; Savage et al., 2017).

Measurements and analyses of bioaerosols can be carried out through different techniques and approaches, each with advantages and limitations, as discussed in the systematic review of Huang and colleagues (Huang et al., 2024). These approaches can be broadly grouped into: (i) culture-based active sampling followed by colony-forming unit enumeration; (ii) volumetric or impactor-based sampling followed by optical, electron or fluorescence microscopy; (iii) molecular methods, including Polymerase Chain Reaction (PCR), quantitative PCR (qPCR), digital PCR (dPCR) and Next-Generation Sequencing (NGS); (iv) flow-cytometry-based approaches; and (v) real-time optical instruments, including Ultraviolet Light-Induced Fluorescence (UV-LIF)-based sensors. The first two represent some of the most traditional methods, consisting of the collection through gravimetric or volumetric impaction on adhesive substrate, such as agar coated dishes or sticky tape, or also onto liquid medium, followed by the cultivation or optical, electron or epifluorescence microscopy. Examples of these techniques are the sampling through a Surface Air System (SAS), cultivation and count of Colony Forming Units (CFU), and sampling on a tape through a volumetric trap (e.g., Hirst-type trap, the standard EN 16868:2019), followed by Optical Microscopy (OM) analysis and count. Generally, these off-line approaches are relatively cost-effective and generally considered the standard for the qualitative and quantitative evaluation of bioaerosols. However, they are usually time-consuming and labour intensive, requiring highly skilled operators. Additionally, some techniques allow only the measurement of viable bacteria and fungal spores, which require specific culture media, and enable sampling of limited air volumes over short periods or, in the opposite, provide low temporal resolution. Moreover, among off-line techniques, molecular methods, such as the PCR or qPCR and the NGS can also be employed. These methods are highly sensitive but are also highly time- and resource-consuming. Flow Cytometry is another off-line approach, based on the light-scattering and fluorescence-emission principles. The fluorescence emission principle is also exploited in direct-reading instruments, based on the UV-LIF. These types of innovative instruments (spectrometers) represent a sort of complementary alternative to off-line techniques, since they allow for real-time monitoring, with a consequent high temporal resolution. However, they do not provide information on the specific type of bioaerosol, therefore requiring additional analytical steps for proper classification. In summary, these approaches provide complementary information: offline methods support taxonomic or viability-related characterization, whereas UV-LIF instruments provide high-time-resolution proxies of fluorescent biological aerosol particles but generally require additional data treatment and/or offline validation for biological attribution.

1.2. LIF-based approach and instruments

LIF-based spectrometers work on the principle that biological particles emit fluorescence when they are irradiated with ultraviolet light. This occurs due to the intrinsic fluorescence (also known as autofluorescence) which arises from naturally occurring bio-fluorophores (i.e., fluorescence molecular components) within the bioaerosols (Fennelly et al., 2017), such as amino acids (e.g., tryptophan, tyrosine and phenylalanine), co-enzymes and vitamins (e.g., nicotinamide adenine dinucleotide (NADH) and nicotinamide adenine dinucleotide phosphate (NADPH)), structural biopolymers and cell wall compounds (e.g., cellulose, chitin and lignin), pigments, secondary metabolites and nucleic acids (i.e., deoxyribonucleic acid (DNA) and ribonucleic acid (RNA)) (Fennelly et al., 2017; Pöhlker et al., 2012). Each bio-fluorophore has an

excitation and emission wavelengths range (in terms on nanometres – nm), which is exploited by the UV-LIF spectrometers to detect bioaerosols. For example, NADH and NADPH are excited at 290-295 nm and 340-366 nm, respectively and both emit at 440-470 nm. Instead, amino acids are excited at 260-295 nm and emit at 280-360 nm. Nevertheless, as reported by Pöhlker and colleagues (Pöhlker et al., 2012), fluorescence is a phenomenon observed across a wide range of chemical compounds and materials, not only for biological materials, such as humic-like substances (HULIS), secondary organic aerosols (SOA), mineral(s) dust, polycyclic aromatic hydrocarbons (PAH) and soot. This means that non-biological (including anthropogenic) aerosols can also emit fluorescence, acting as interferents that can lead to false-positive detections and must therefore be carefully considered during data interpretation. Currently, some of the most widely used commercially available instruments include different versions of the Wideband Integrated Bioaerosol Sensor (WIBS) and the Rapid-E. Although based on a similar conceptual approach and developed for the same purpose, these instruments differ substantially in the way they characterize fluorescent particles, as described in detail in the Supplementary Material. Briefly, Rapid-E primarily relies on the fluorescence spectrum of individual particles, obtained by measuring fluorescence intensity across multiple wavelengths, and additionally provides information on particle size and fluorescence lifetime. In contrast, the WIBS characterizes particles in terms of size, shape through the asphericity factor (AF), and fluorescence intensity measured in three detection channels (FL1, FL2 and FL3, resulting in the classification of fluorescent particles into types A, B, C, AB, AC, BC and ABC), derived from the combination of two excitation sources and two detectors operating over different emission wavelength ranges. Details of operating principles and technical specifications are reported in Supplementary Material [Tables SM1 and SM2].

1.3. Aims of the study

As mentioned before, UV-LIF instruments are relatively recent, especially compared to the traditional approaches which are still widely used. To the best of authors' knowledge, only one scientific review is currently available in the literature, published in 2017 by Fennelly and colleagues (Fennelly et al., 2017), which focuses on the BioScout, UV-APS and WIBS instruments. More specifically, for the latter, only the WIBS-3, WIBS-4, and WIBS-4A versions were explored, since at that time no peer-reviewed papers were available on WIBS-5/NEO. Therefore, an update concerning this latter version, along with a first exploration of the analogous Rapid-E and Rapid-E+ instruments (hereafter referred as Rapid-E(+) when referring collectively to Rapid-E and Rapid-E+, and use Rapid-E or Rapid-E+ only for specific versions), is valuable for addressing the gap in scientific knowledge regarding their application in laboratory studies, indoor and outdoor environments. A further aim was to synthesize data-treatment strategies, validation approaches and practical applicability of WIBS and Rapid-E(+) to support more standardized and decision-oriented use of UV-LIF bioaerosol monitoring.

2. Materials and methods

A systematic review of the literature was performed following PRISMA guidelines (Page et al., 2021). In detail, a query was developed to retrieve the original articles resulting from the search on Scopus, Web of Science and PubMed databases. The query was built considering two topics: (i) biological aerosols, including bacteria, viruses, fungi and pollen, and (ii) instruments of interest for the real-time monitoring of bioaerosols (i.e., different versions of WIBS and Rapid-E(+)). In the present review, Rapid-E(+) is used as an umbrella term for Rapid-E and Rapid-E+ studies. Rapid-C-related terms were retained in the search strategy to maximize sensitivity, but no Rapid-C study met the final eligibility criteria within the scope of this review. The search strategy was based on two mandatory concept blocks: (i) instrument-related terms, to capture studies using WIBS or Rapid-E platforms, and (ii) broad bioaerosol-related terms, including both general descriptors (e.g., "bioaerosol*", "biological", "microorganism*", "microbi*") and terms referring to major biological particle classes (e.g., bacteria, viruses, fungi, spores, moulds, yeasts and pollen). Very broad terms such as "pathogen*" and "bio-pollution" were not included in the primary string because they were considered less specific to UV-LIF bioaerosol monitoring and more likely to increase retrieval of non-relevant records. The list of keywords was arranged in queries [Table 1] following the writing rules required for each database.

As reported in the flow chart [Fig. 1], an initial search was performed on 19th February 2024 and an update was carried out on 23rd July 2025, prior to manuscript preparation. The search on databases was limited to the English-written original articles, and no other restrictions were adopted (e.g., no geographical or temporal filters were applied). Articles resulting from the searches were included if they (a) concerned any version of WIBS or Rapid-E(+), and (b) reported results from laboratory measurements or data analyses, or presented data obtained during in-field monitoring campaigns aimed to assessing characteristics (e.g., concentration, size and shape, temporal trends) of biological agents. If the study concerned fluorescent particles but did not consider them as proxies for bioaerosols, they were discarded. A total of 76 original articles met the inclusion criteria and were selected for this review. Outcomes emerging from the studies were schematically organized in a dedicated database by two authors according to the structure defined *a priori* for the paragraph of Results: "3.1. Framing of the included articles", to provide an overview of the applications of these instruments in different types of studies; "3.2. Laboratory studies", concerning the main results emerging from studies performed under controlled conditions or concerning data analysis are presented; "3.3. Indoor field studies" and "3.4. Outdoor field studies", including results about concentrations (in terms of average, median, interquartile, etc.), characteristics and temporal trends from monitoring campaigns performed indoors and outdoors, respectively; "3.5. Comparisons with other instruments", in which the outcomes concerning comparisons with other instruments for bioaerosol detection are reported, mainly based on correlations and concentration levels. A formal quantitative meta-analysis was not performed because the included studies were highly heterogeneous in terms of instrument version, operational mode, particle size range, fluorescence threshold, target bioaerosol, reference method, temporal aggregation and reported performance metrics. Instead, we performed a structured narrative and semi-quantitative

Table 1
Queries used for the original articles research in Scopus, Web of Science and PubMed.

Database	Search Query
Scopus	TITLE-ABS-KEY ("WIBS-5/NEO" OR "WIBS-5″ OR "WIBS*" OR "Rapid-E+" OR "Rapid-C″ OR "Rapid-E″) AND TITLE-ABS-KEY ("bioaerosol*" OR "bacter*" OR "virus*" OR "fung*" OR "spor*" OR "mold*" OR "mould*" OR "yeast*" OR "biological" OR "microorganism*" OR "microbi*"OR "pollen*" OR "bioparticle*" OR "bio-particle*")
Web of Science	TS=("WIBS-5/NEO" OR "WIBS-5″ OR "WIBS*" OR "Rapid-E+" OR "Rapid-C″ OR "Rapid-E″) AND TS=("bioaerosol*" OR "bacter*" OR "virus*" OR "fung*" OR "spor*" OR "mold*" OR "mould*" OR "yeast*" OR "biological" OR "microorganism*" OR "microbi*" OR "pollen*" OR "bioparticle*" OR "bio-particle*")
PubMed	("WIBS-5/NEO"[Title/Abstract] OR "WIBS-5"[Title/Abstract] OR "WIBS*"[Title/Abstract] OR "Rapid-E+"[Title/Abstract] OR "Rapid-C"[Title/Abstract] OR "Rapid-E"[Title/Abstract]) AND ("bioaerosol*"[Title/Abstract] OR "bacter*"[Title/Abstract] OR "virus*"[Title/Abstract] OR "fung*"[Title/Abstract] OR "spor*"[Title/Abstract] OR "mold*"[Title/Abstract] OR "mould*"[Title/Abstract] OR "yeast*"[Title/Abstract] OR "biological"[Title/Abstract] OR "microorganism*"[Title/Abstract] OR "microbi*" [Title/Abstract] OR "pollen*"[Title/Abstract] OR "bioparticle*" [Title/Abstract] OR "bio-particle*"[Title/Abstract])

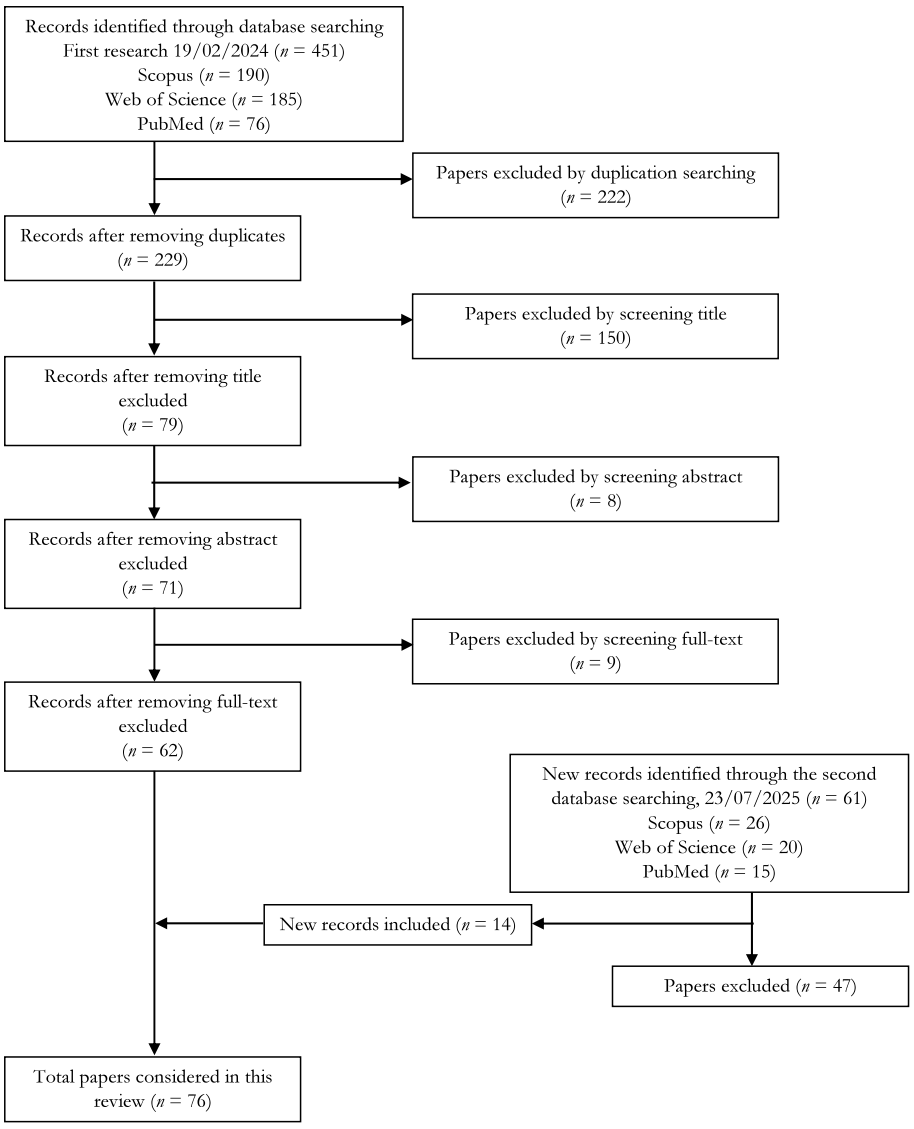

Fig. 1. Flowchart of the selection of the papers included in this review.

synthesis supported by evidence maps, comparative tables and decision matrices. To complete the descriptive synthesis, a bibliometric visualization of the 76 included articles was performed using metadata extracted from the final RIS file exported from Zotero, after merging records retrieved from the aforementioned bibliographic sources. Author names were manually checked and harmonized to reduce inconsistencies due to spelling variants, initials, accents and apostrophes. In addition, keywords and recurrent title/abstract terms were normalized using a controlled list of semantically equivalent terms and acronyms. Publication year was used to describe temporal trends. Co-authorship relationships were explored to identify collaboration clusters among recurrent authors, while keyword/term frequency and co-occurrence were used to summarize the main thematic areas covered by the included literature. Co-authorship and keyword/term co-occurrence networks were generated using Python and NetworkX, and communities were identified using greedy modularity optimization. Visualization thresholds were applied to improve readability and are reported in Fig. 2. Since no statistical synthesis were performed, the risk of bias in the included studies was not assessed, as well as heterogeneity and sensitivity analyses. Also, due to the descriptive nature of the evidence and the absence of statistical synthesis no formal certainty grading was applied.

3. Results

3.1. Framing of the included articles

Table SM3 reports the complete list of the 76 studies included in this review (76 original articles, corresponding to 79 instrument-specific study records because three studies investigated both WIBS and Rapid-E(+)), indicating the specific sections in which each article is discussed. A general overview of the included papers is provided in Figs. 2 and 3, and Table SM4. Fig. 2 provides an evidence map of the 76 included original articles, classified by instrument version and review section, meanwhile Table SM4 summarizes the number of publications concerning WIBS and Rapid-E(+) instruments by publication year. Because three studies investigated both WIBS and Rapid-E(+), the number of instrument-specific records is higher than the number of original articles. Overall, a lack of homogeneity is observable. The number of published papers has slightly increased in recent years, with most of them focusing on WIBS instruments (n = 63, since 2010) and a smaller fraction addressing the Rapid-E(+) (n = 16, since 2019), in the year after their market release. Also, most of the instruments were used in outdoor field studies (n = 51), followed by laboratory studies (n = 32). A considerable number of studies provided comparisons with other

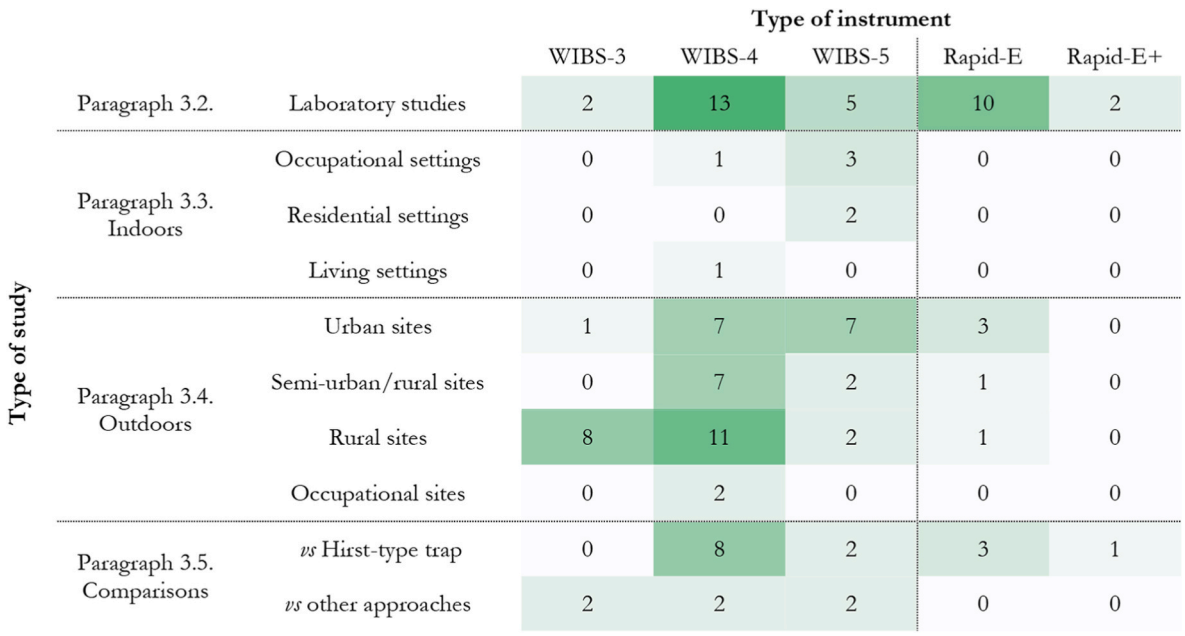

Fig. 2. Evidence map of the included original articles by review section and instrument type and version. Numbers refer to articles or instrument-specific study records contributing to each section; articles may contribute to more than one section.

bioaerosol measurement instruments (n = 20), whereas only a limited subset involved measurements in indoor environments (n = 7), all of which regarding the use of WIBS.

The supplementary bibliometric visualization provided an overview of the temporal, collaborative and thematic structure of the 76 included records [Fig. 3]. Coherently with Table SM4, the publication timeline showed a progressive increase in studies from 2010 onward, with a higher number of records in recent years. The co-authorship network highlighted a limited number of recurrent collaboration clusters, reflecting the presence of specialized research groups working on UV-LIF-based bioaerosol monitoring. The most frequent normalized terms were related to UV-LIF/fluorescence, bioaerosols/PBAP, WIBS, meteorology, real-time monitoring, fungal spores, calibration/validation, pollen, classification and outdoor/ambient air. The co-occurrence map confirmed that the literature is mainly organized around methodological and instrumental aspects, biological particle classes, environmental/meteorological drivers, and data treatment/classification approaches.

3.2. Laboratory studies

3.2.1. WIBS instruments

In this paragraph, the main outcomes from laboratory studies using WIBS instruments are presented, dividing results concerning evaluation of performance tests (i.e. efficiency of particle count, size classification, biological particle type discrimination) and post-processing of data.

Two studies assessed the dimensional counting efficiency of a WIBS-4 (Healy et al., 2012a) and a WIBS-NEO (Lieberherr et al., 2021) using standard monodisperse polystyrene latex (PSL) spheres of different sizes as standard samples and comparing counting performance with reference instruments: a Condensation Particle Counter (CPC) and an Optical Particle size (OPC) primary standard, respectively. For smaller particle sizes, results were broadly in agreement between the studies, with a counting efficiency of 50% around 0.5 μm, increasing to 100% for particles of about 1 μm. However, with the WIBS-NEO larger particles were also tested and it provided robust measurements up to 2 μm, followed by a strong decrease in counting efficiency (down to 4% for particles with a diameter of 10 μm). According to the work of Savage and colleagues (Savage et al., 2017), significant sizing errors can be introduced by the internal calibration of WIBS; therefore, a calibration should be performed before any analysis to obtain representative data. Some calibration procedures were performed and described (Robinson et al., 2017; Savage et al., 2017), both for size and fluorescence instrumental responses. In these studies, for each sample (including biological and non-biological materials) a histogram of particle size or fluorescence intensity signal was plotted and fitted with a Gaussian function to retrieve each median value and thus obtain a calibration function. Notable, Robinson and colleagues (Robinson et al., 2017) tested the role of the detector gain voltage. Authors observed that a higher voltage leads to a higher response, which is useful when the goal is to maximize detection of small amounts of fluorescent material, but in the other hand it results in a lower saturation threshold, leading to a loss of fluorescence intensity information for strongly fluorescent particles.

Most of the other laboratory studies were focused on testing the performance and ability of WIBS instruments in discriminating between biological and non-biological aerosols (Forde et al., 2019b; Healy et al., 2012b; O'Connor et al., 2013; Santander et al., 2021; Savage and Huffman, 2018; Toprak and Schnaiter, 2013a). More in detail, these studies typically provided measurement of samples that were separately aerosolized in a chamber, for which data related to fluorescence intensity (in the three WIBS detection channels: FL1, FL2, FL3), size and AF were retrieved. Different approaches for data comparisons were adopted, either just considering the fluorescence intensity measured in each channel (Santander et al., 2021; Savage and Huffman, 2018; Toprak and Schnaiter, 2013a) or by calculating ratios between fluorescence intensities across channels and/or with particles size (e.g., FL3/FL1 or FL1/size) (Forde et al., 2019b; Healy et al., 2012b; O'Connor et al., 2013), and using different two-dimensional (2D) or three-dimensional (3D) graphical representations. However, regardless the adopted data analysis approach, WIBS instruments have shown good performances in discriminating between PBAPs and non-PBAPs based on fluorescence intensity measurements, even though some interferents could provide for false-positive. Good performances were also observed for the discrimination among different bioaerosols. Generally, different fluorescence signals can be measured by different instruments (especially when considering different versions). However, it was observed that bacteria display dominance in the FL1 channel, while pollens tend to exhibit fluorescence across all channels. Instead, fungal spores seem to provide more variable outcomes, with fluorescence dominance

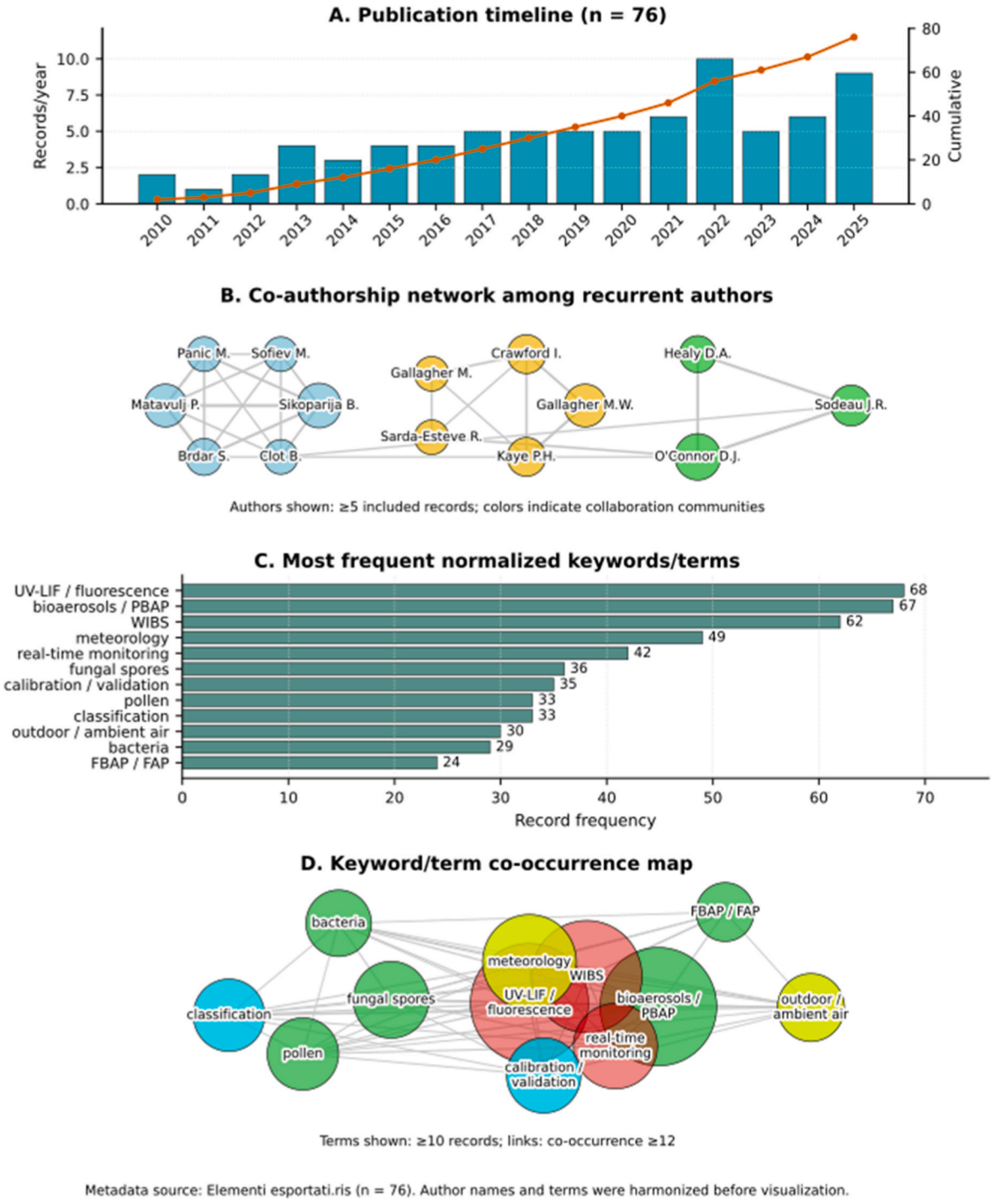

Fig. 3. Bibliometric visualization of the 76 records included in the systematic review. (A) Publication timeline, showing the annual number of included records and the cumulative number of records over time. (B) Co-authorship network among recurrent authors. Nodes represent authors occurring in at least five included records; node size is proportional to the number of included records; edges represent co-authorship links; colors indicate modularity-based collaboration communities. (C) Frequency of the most recurrent normalized keywords/terms. Frequencies refer to normalized terms after manual harmonization and should not be interpreted as raw keyword occurrences. (D) Co-occurrence map of normalized keywords/terms extracted from title, abstract and keyword fields. Node size is proportional to the number of records in which the term occurs; edges represent co-occurrence within the same record; colors indicate term communities. Author names, acronyms, spelling variants and semantically equivalent terms were harmonized before visualization. (For interpretation of the references to color in this figure legend, the reader is referred to the Web version of this article.)

differing among the channels (Forde et al., 2019b; Healy et al., 2012b; Zhang and Lai, 2025). Healy and colleagues (Healy et al., 2012b) observed a good degree of separation between fungal spores and pollen, when plotting 3D graphs (FL1/FL3/size, and FL2/FL3/size), especially with the FL1/FL3 channels, providing the potentially of WIBS in distinguish natural airborne PBAP samples. Conversely, when considering different pollen taxa, more difficulties emerged since they provided an identical number-size distribution in each channel, probably due to the saturation of the detector. Notably, fluorescence intensity can be affected by particle size, generally increasing with increasing size

(Forde et al., 2019b; Savage and Huffman, 2018). Hence, this parameter should be considered in the data analysis, may calculating the ratio between fluorescence intensity and size (FL/size), as previously described. Another possible issue occurring with pollens is due to their fragmentation, which can lead to a reduction in the size (Forde et al., 2019b). Venkatesan and colleagues (Venkatesan et al., 2025) replicated the interactions between pollen and humidity by exposing airborne pollen to both ambient atmospheric and elevated humidity levels, to evaluate the changes in pollen size due to the breakdown caused by osmotic forces (which can affect health effects due to closer interactions with the upper respiratory tract). It emerged that the exposure to high humidity levels can lead to the rupture of pollen particles, although it was not recorded for all tested species. Another interfering factor in LIF-based bioaerosol monitoring could be the particle aging due to the exposure to sunlight (especially UV radiation) and ozone. Especially, the exposure of bacteriophages to simulated sunlight and ozone has been shown to cause a significant decrease in fluorescence signal (Ackerman et al., 2025).

Other laboratory studies have explored the capability of various clustering techniques in identify the nature of fluorescence particles, like Hierarchical Agglomerative Cluster Analysis (HACA), Density Based Spectral Clustering and Noise (DBSCAN), k-means and gradient boosting (Crawford et al., 2015; Robinson et al., 2013; Ruske et al., 2018; Savage and Huffman, 2018). These approaches were tested on different datasets, including both laboratory and environmental measurements, performed with WIBS-3 or WIBS-4(A). Cluster analysis resulted the most explored technique, although methodological differences exist across studies regarding preprocessing, linkage criteria, distance metrics, and the method used to define the optimal number of clusters (details are reported in Table SM5). In the study of Robinson and colleagues (Robinson et al., 2017) data were normalized using z-score, and clustering were performed through the average linkage and Euclidian distance. This attribution algorithm resolved much of the laboratory (PSLs) data, provided consistent results between two ambient datasets, and appeared to resolve some aerosol types (i.e., accumulation mode aerosol, bacterial clusters, fungal smut spores and other fungal spores). The effectiveness of this approach is further supported by the study of Crawford and colleagues (Crawford et al., 2015), in which several cluster analysis algorithms were tested on both a laboratory and an ambient dataset. According to the results, data can be successfully separated using the Ward's hierarchical agglomerative cluster analysis linkage, with z-score and range data normalization. However, these finding contrasted with those of Savage and Huffman (2018), who reported that the highest-quality clustering was achieved without fluorescence normalization (instead of z-score normalization), but using log-transformed variables. This algorithm provided a general good separation between PBAP and non-PBAP, using a fluorescence threshold of 3σ, but lower performance when considering a trial with two biological particle types. Ruske and colleagues (Ruske et al., 2018) tested a total of 96 different approaches. According to the authors, the same approach provided by Crawford and colleagues (Crawford et al., 2015) did not always provide the best performance, but it was found to be consistent across different datasets, thus, "it becomes difficult to provide a better recommendation". Moreover, in this latter study, k-means, gradient boosting and DBSCAN were also evaluated. Gradient boosting consistently offered the best performance across the different data preparation and datasets. It was observed that data preparation had a very small impact upon performance, as long as some kind of fluorescence threshold is applied where a high value of the adjusted rand score was obtained. On the contrary, k-means performed poorly, leading the authors to omit its results. Regarding DBSCAN, one of the main challenges lies in selecting the minimum number of points to form a neighbourhood and its radius (ε): among the different repetitions the best results were obtained by setting the number of points between 0.4% and 0.7% respect to the total of data when using an $\varepsilon = 0.3$ (9σ) and 0.7% and 1.0% when using an $\varepsilon = 0.4$ (3σ).

Finally, among these laboratory studies, two of them (Xie et al., 2024; Zhou et al., 2017) investigated human emission rates of bioaerosols (with WIBS-4A), under controlled conditions. Zhou and colleagues (Zhou et al., 2017) assessed the impact of two relative humidity conditions (40-45% and 60-70%) and two skin moisturizer states (with and without application) using a 2×2 experimental design, in a small office room. The authors observed that under high relative humidity (RH) and without moisturizer, the mean emission rate of total fluorescent aerosol particles ranged in 6.8-7.5 $\times 10^6$ particles/person/hour, with ABC, A and AB particle types accounting for more than 90%, and most in the size range of 1-5 μm. At lower RH, no significant changes were observed; however, the use of skin moisturizer led to an increase in emission rates, ranging approximately (according to the graphs in the original paper) between 20 and 30 $\times 10^6$ particles per person per hour, mainly due to particles in the 1-2.5 μm size range. Instead, Xie and colleagues (Xie et al., 2024) explored the emission rates of 12 subjects sat for 45 min, wearing and not wearing a N95 mask. Fluorescent bioaerosols represented a relatively small fraction (approximately 1–3%) of the total aerosols emitted by the human body and did not exhibit significant variations between wearing and not wearing masks. No significant differences were observed comparing the two conditions for fluorescent particles in the 0.5-2.5 μm size range, with average emission rates of 3.19 $\times 10^4$ and 3.07 $\times 10^4$ particles/person/h, without wearing and wearing a mask, respectively. Instead, in the 2.5-10 μm size range, the average emission rate was 13.98 $\times 10^4$ particles/person/h without wearing the mask, which increased to 20.64 $\times 10^4$ particles/person/h with mask. These results suggested that during periods of prolonged sitting, bioaerosols released through skin metabolism and other bodily processes exhibited higher emission rates, whereas bioaerosols generated through respiration had a minor impact. As observed, the magnitude of emission rates differed considerably between the two studies, which is likely attributable to differences in study design, involving physical movement in the first case and sedentary conditions in the second.

In summary, laboratory studies demonstrate that WIBS instruments achieve robust performance in detecting particles in the finest fraction, especially at ~1 μm, while performance for coarser particles and sizing accuracy strongly depend on instrumental calibration and operating settings. WIBS laboratory studies indicate that fluorescent biological and non-biological particles can often be separated under controlled conditions, also with good results obtained in discrimination between PBAPs and non-biological fluorescent interferents, and, in several cases, among different biological particle types. However, performance and fluorescence response are strongly affected by fluorescence thresholds, particle size and aging processes, environmental conditions, detector settings, calibration procedures and pre-processing choices. Therefore, laboratory separability should not be directly interpreted as robust field-level biological attribution without independent validation (Ackerman et al., 2025; Forde et al., 2019a; Healy et al., 2012a; Robinson et al., 2017; Ruske et al., 2018; Savage et al., 2017). The application of multivariate and machine-learning (ML) approaches enhances classification capabilities, although variability in preprocessing strategies, clustering methods and training datasets leads to heterogeneous outcomes across studies, highlighting the need for standardized analytical frameworks and cross-study validation.

3.2.2. *Rapid-E(+) instruments*

A lower number of laboratory studies concerned the use of Rapid-E (+). Among these, only one study (Lieberherr et al., 2021), which also involved a WIBS instrument as already discussed in the previous section, evaluated the dimensional counting efficiency of a Rapid-E using different dry aerosolized PSL spheres. Results indicated that Rapid-E detect larger particles more effectively. In detail, compared with a CPC, the instrument showed a counting efficiency of 58%, 42% and between 1 and 4% for particles of 10 μm, 5 μm and 2 μm in diameter, respectively. At 1 μm, almost no PSLs were detected. The authors also

calculated the root mean square error deviation (RMSD) between the scaled reference and Rapid-E to assess the scalability of the measurements, reporting a RMSD of 25-29% for particle with a diameter of 2-10 μm, and of 89% for the 1 μm particles. Concerning the particle size determination, the authors observed a well-defined peak for 5 μm particles, while a broader one for the 10 μm particles, suggesting that more particles were detected as finer or coarser. Finally, the authors compared the fluorescence response of Rapid-E after excitation of three different 2 μm PSL spheres (blue, plum purple, and red) with reference data from the Max Planck Institute for Chemistry. Rapid-E fluorescence spectra corresponded relatively well to the reference spectra, although a higher signal-to-noise ratio was observed for red PSL particles. Beyond this instrumental evaluation, all the other studies explored different approaches for the classification of fluorescent particles as biological aerosols, mainly based on deep machine learning. Given the complexity and breadth of ML approaches, the following section summarizes the main types of neural networks architectures adopted and, when relevant, the characteristics and configurations of the algorithms. For further details, please refer to the original articles. Among the techniques used for pollen and fungal spores classification, Convolutional Neural Network (CNNs) (Boldeanu et al., 2021; Brdar et al., 2023; Bruffaerts et al., 2025; Daunys et al., 2024; Matavulj et al., 2022, 2023; Sikoparija et al., 2024; Tešendić et al., 2020) and Artificial Neural Network (ANNs) (Boldeanu et al., 2022; Šauliene et al., 2019) were most frequently implemented, possibly in combination with other methods. These models were trained and tested on various datasets consisting of scattering and fluorescence signals of biological and non-biological aerosols. Different filters and pre-treatments were applied to the Rapid-E data prior to testing the performance of these various CNN and ANN algorithms. Overall, it was observed that performance increased when combining more input data (e.g., scattering, fluorescence spectrum and lifetime) (Brdar et al., 2023; Daunys et al., 2021, 2024; Matavulj et al., 2023; Šauliene et al., 2019). Especially, Daunys and colleagues (Daunys et al., 2024) (in which Vision Transformers architectures and a WSOD – Weakly Supervised Object Detection – Wildact were also considered in addition to CNNs) observed that simple methods are faster, but less accurate. Boldeanu and colleagues (Boldeanu et al., 2022) obtained a reduction of the relative error rate through an extensive hyperparameter search, and Daunys and colleagues (Daunys et al., 2021) observed that combining scattering and fluorescence data proved more effective than using either alone, by applying an agglomerative clustering approach combined with neural networks to evaluate the effectiveness in discriminating different species of pollen taxa (20 woody and 9 herbaceous). Anyway, caution is required with more sophisticated methods because the higher complexity (which requires more time) does not necessarily correspond to proportional gain in accuracy (Daunys et al., 2024). Generally, these approaches achieved good performance in discriminating among different pollen taxa. With the Rapid-E version, an average accuracy of 63% (ranging between 29.7% and 86.1%, in discriminating 12 pollen classes) and of 65.3% (in discriminating 24 pollen classes and 2 non-biological aerosols) were reached by Brdar and colleagues (Brdar et al., 2023) and Tesendic and colleagues (Tešendić et al., 2020), respectively. Higher performances were obtained by Sauliene and colleagues (Šauliene et al., 2019), with accuracies of 73%, 74% and 80% for three similar but distinct datasets, composed by 11, 14, 10 pollen samples, respectively, while Boldeanu and colleagues (Boldeanu et al., 2022) achieved an accuracy up to 87% with CNNs, after hyperparameter tuning, and 72% with a Multilayer Perceptron (MLP, a type of ANN).

Consistent results were also obtained with the Rapid-E+. Sikoparija and colleagues (Sikoparija et al., 2024) trained a ResNet-based algorithm on an extensive training dataset (27 pollen species) performing the laboratory measurements in two different sensitivity modes: “pollen mode” and “middle mode”. High performances (precision = 94%, recall = 98% and F1 score = 0.96) were achieved by the binary model, which discriminated pollen from “other” bioaerosols, and with the instrument set on “pollen mode”. Good performances were also obtained in discriminating among the 27 pollen classes with the instrument in “pollen mode”, with average precision, recall, and F1 score of 83%, 85% and 0.84, respectively, slightly improving to 86%, 86% and 0.86 after merging 4 pollen species previously misclassified. Instead, in “middle mode”, binary classification performance slightly decreased (precision = 93%, recall = 96%, F1 = 0.95), while multiclass performance dropped to 75%, 77%, and 0.76. Bruffaerts and colleagues (Bruffaerts et al., 2025) achieved an accuracy ranging between 83.4% and 95.1% across 17 fungal species, with the Rapid-E+ operating in “middle mode” and adopting a ResNet architecture integrating multiple measurements modalities for the classification (i.e., parallel and perpendicular polarization scattering, infrared scattering, fluorescence spectrum, and fluorescence lifetime data). Although these results are generally comparable, inter-study and intra-study variability in performance are notable. These differences can be attributed to the use of different datasets which were built with different calibration, experiments performed with both different pollen samples and Rapid-E(+) devices. As emerged in some studies (Boldeanu et al., 2021, 2022; Brdar et al., 2023), some pollen classes are easily separable while others remain challenging. Moreover, Boldeanu and colleagues (Boldeanu et al., 2022) found that inter-dataset errors suggested overfitting to specific devices, a phenomenon further supported by Sikoparija and colleagues (Sikoparija et al., 2024) and Matavulj and colleagues (Matavulj et al., 2022), who observed a drastic drop in classification performance (according to F1 score) when applying a model trained on one Rapid-E(+) unit to another device or on a reference dataset from another device. However, Matavulj and colleagues (Matavulj et al., 2022) also explored the possibility to add some missing classes from an external dataset, and the authors observed that the implementation of domain adaptation allows to improve the classification of a reference dataset from the other device.

Overall, according to laboratory studies, Rapid-E(+) displayed a limited detection efficiency for particles lower than 2 μm, which is better for the coarsest fraction. While fluorescence measurements show good agreement with reference spectra, particle size determination and counting accuracy remain size-dependent. The application of advanced machine-learning approaches has demonstrated good performance in classifying pollen, fungal spores and other bioaerosols, particularly when multiple scattering and fluorescence features are combined. In this context, Rapid-E(+) studies benefit from richer particle-level information, including fluorescence spectra, lifetime and scattering-related features, supporting more advanced supervised classification, particularly for pollen and fungal spores. However, performance depends strongly on the representativeness, transferability and quality of training datasets, as well as by calibrations procedures, instrument settings and device-specific response, contributing to substantial inter- and intra-study variability (Boldeanu et al., 2021, 2022; Brdar et al., 2023; Matavulj et al., 2023; Sikoparija et al., 2024).

3.3. Indoor field studies

As mentioned before and outlined in Fig. 2, indoor environments were investigated only using WIBS instruments. In detail, occupational settings (n° of studies = 4), residential settings (n° of studies = 2), and a living setting (n° of studies = 1) were involved. From an exposure-assessment perspective, indoor WIBS studies show that high-time-resolution UV-LIF data are particularly useful for identifying occupancy-, activity- and ventilation-related changes in fluorescent particles. However, these signals should be interpreted as real-time proxies rather than taxonomic measurements, especially where human emissions, resuspension and outdoor infiltration occur simultaneously (Addor et al., 2022; Lancia et al., 2023; Li et al., 2022; Wingert et al., 2022; Xie et al., 2017; Zhou et al., 2017).

3.3.1. WIBS instruments

3.3.1.1. Occupational settings. Li and colleagues (Li et al., 2022), Lancia and colleagues (Lancia et al., 2023) and Xie and colleagues (Xie et al., 2017) performed measurements in offices. High concentrations of fluorescent and non-fluorescent particles during occupancy periods were observed (Lancia et al., 2023; Li et al., 2022). Lancia and colleagues (Lancia et al., 2023) measured average daily numbers of FAPs (Fluorescent Aerosol Particles) of 131,807 on working days and 110,417 on non-working days, although the highest value (198,500 daily fluorescent particles) was observed during a non-working day. Li and colleagues (Li et al., 2022) estimated average FAP mass concentrations of 4.9 μg/m^3 during working hours and of 0.3 μg/m^3 during non-working hours. Moreover, both studies classified FAPs into different bioaerosol types (i.e., bacteria, fungi, pollen), according to similar criteria based on fluorescence channel and particle size [Table 3]. Consistent with the fluorescent particles trend, Li and colleagues (Li et al., 2022) found that bacteria-, fungi- and pollen-like particles showed higher concentrations during occupied periods. Notably, the authors observed a situation in which levels of fluorescent particles (especially the finer fraction) and bacteria-like particles increased before the arrival of occupants, following the HVAC (heat ventilation air conditioning) system activation, which possibly acted as a reservoir for bioaerosol during the nights (when it is turned off). Partly consistent results were obtained by Lancia and colleagues (Lancia et al., 2023), who found that the pollen- and spore-like particle number clearly followed the workers presence, while the number of bacteria-like particles did not vary substantially between working day and non-working days. Conversely, Xie and colleagues (Xie et al., 2017) investigated an office setting only during an unoccupied period and focusing on the size-distribution and AF of FAPs in channel 1 (i.e., FL1). The particle size-distribution displayed a bimodal pattern, with the two peaks occurring at 1.35-1.5 μm and 2.1-2.25 μm. In contrast, AF fit a lognormal distribution, peaking at a value of between 11 and 11.5.

Wingert and colleagues (Wingert et al., 2022) performed a study in three thanatopraxy laboratories to evaluate embalmers' exposure to bioaerosols over a full working day. Concentrations of FAPs varied between 0.25 particles/cm^3 up to 7.65 particles/cm^3, depending on the activity performed. Overall, emissions of biological particles were clearly identifiable during different tasks, but the activities that most exposed workers were those involving bellows effect (i.e. suturing using sealing powder, occlusion, wrapping).

3.3.1.2. Residential settings. Two studies investigated residential environments (Addor et al., 2022; Li et al., 2020). Li and colleagues (Li et al., 2020) performed a nearly month-long monitoring campaign (23rd March - 20th April 2019) inside a naturally ventilated and occupied bedroom in Singapore, located at the 6th floor of a building. Addor and colleagues (Addor et al., 2022) carried out measurements between 6th August and 30th September 2020, during COVID-19 lockdown, inside an inhabited residential apartment (two adults and two children), located on the 3rd floor of a residential building in Ohio (USA). Similar results were obtained by the two studies, with, median and mean fluorescent particle concentrations of 0.70 particles/cm^3 (Li et al., 2020) and 0.98 particles/cm^3 (Addor et al., 2022), contributing to approximately 19% and 24% of total particles, respectively. Li and colleagues (Li et al., 2020) recorded higher concentrations during occupied periods and with closed windows, observing emission rates up to 94.5×10^6 particles/hour. Coherently, Addor and colleagues (Addor et al., 2022) observed peaks coinciding with increased human activity (around 7 a.m. and 11 a.m.), which resulted be a major contributor. Also, they calculated an hourly number-weighted mean diameter of 1.38 μm across the whole monitoring period.

3.3.1.3. Living settings. Fan and colleagues (Fan et al., 2025) investigated FBAPs in a subway station in China, during June 2023, with a WIBS-4A. The subway station consists of four subterranean levels, and indoor measurements were conducted on the second basement level, with an area of 15,600 m^2 and serving the subway hall and office area, and at the fourth basement level, located at the exit of the lower end of the staircase passage, which is subject to intensive airflow from the ventilation system and train movements. According to the results, most particles had a diameter smaller than 2.5 μm, with distinct peaks observed during both the morning and evening rush hours, and higher concentrations detected on the platform compared to the hall.

Overall, although only a limited number of studies have investigated indoor environments across occupational, residential and public settings, they consistently highlight the strong influence of human presence and activities on fluorescent particles and bioaerosols. An additional relevant finding is the potential role of HVAC systems, which may act as secondary sources of biological agents.

Table 2
Criteria adopted for the classification of fluorescent particles in bioaerosols (i.e., bacteria, fungi and pollen), by Li and colleagues (Li et al., 2022) and Lancia and colleagues (Lancia et al., 2023).

(a) Classification criteria of fluorescent particles for defining bioaerosol in the study of Li and colleagues

	Bacteria-like	Fungi-like	Pollen-like
Size range	0.5 – 1.9 μm	2 – 10 μm	1.2 – 10 μm
Type A contribution	91%	80%	6%
Type B contribution			4%
Type C contribution			6%
Type AB contribution	9%	15%	
Type BC contribution			
Type AC contribution			34%
Type ABC contribution		5%	50%

(b) Classification criteria of fluorescent particles for defining bioaerosol in the study of Lancia and colleagues

	Bacteria-like	Fungi-like	Pollen-like
Size range	<2 μm	2 – 10 μm	>10 μm
Type A	X	X	
Type B			
Type C			X
Type AB		X	
Type BC			X
Type AC			
Type ABC			X

3.4. Outdoor field studies

3.4.1. WIBS instruments

A lot of studies (n = 43) focused on measurements performed with WIBS instruments in different outdoor environments. For the sake of clarity, outcomes emerging from these works were grouped according to the type of site investigated (as described in the original articles): urban, semi-urban/rural, rural, and occupational. This categorization was adopted to facilitate comparisons across studies and to highlight differences between the various environments. Outdoor and urban studies differed not only in geographical and meteorological context, but also in the level of data interpretation applied to UV-LIF signals. Some studies reported descriptive FAP/PBAP number or mass concentrations, whereas others applied size- and channel-based filtering, fluorescence thresholds, clustering or supervised machine-learning approaches. This distinction is critical because agreement with reference methods was generally driven more by data-treatment choices than by raw fluorescent particle counts alone. Given this heterogenicity across a large number of original papers, the main data-treatment approaches, their strengths, limitations and practical recommendations are summarized in Table 3, while comprehensive tables with references and available data on concentrations, size and shape of fluorescent particles (explicitly

Table 3
Application-oriented synthesis of evidence for WIBS and Rapid-E(+) in bioaerosol monitoring.

Application context	Instrument(s)	Evidence base synthesis in the reviewed literature	Data-treatment approach reported or implied	Main methodological limitation
Laboratory studies for bioaerosol identification/ discrimination	WIBS and Rapid-E(+)	Good distinction between biological and non-biological species. Fine-level taxonomic discrimination more uncertain and labor-intensive than low-level classification, which generally provides better performance	· Size and fluorescence filtering · Fluorescence classification · Multivariate analysis and machine learning methods	False-negative or false-positive assignments due to: - weak or variable autofluorescence - metabolic state - matrix effects - non-biological interferents
Indoor, residential and occupancy-related studies	WIBS	Use of WIBS/UV-LIF for: - high-time-resolution assessment of occupancy- and activity-related particle events - indoor/outdoor dynamics - source/event tracking	· Time-series analysis · Size-resolved classification, activity logs · Paired indoor/outdoor measurements and ratios	· Limited taxonomic attribution · Possible overlap of indoor activities, human shedding, ventilation and outdoor infiltration
Long-term outdoor/ ambient FAP-PBAP monitoring	Primarily WIBS, and also Rapid-E+	Characterization of fluorescent aerosol concentrations, morphology, spatial–temporal patterns, and source/event dynamics across urban to remote environments, rather than direct taxonomic identification.	· Size and fluorescence filtering · Fluorescence classification · Temporal-pattern analysis · Clustering in selected studies	· FAP/FBAP signals may include non-biological fluorescent particles · Interpretation depends on thresholds, site context and validation
Urban, haze, biomass-burning, dust and rain events	WIBS	Interpretation of fluorescent particle signals in urban and polluted atmospheres requires integration with PM, black/elemental carbon, chemical composition, meteorology and air-mass analysis to account for co-pollutants, dust and combustion-related interferences.	· Conservative thresholding · Size filtering · Fluorescence classification, co-pollutant/meteorological analysis · Trajectory or source-receptor analysis · Sensor-fusion approaches	Non-biological fluorescent interferents may mimic biological fluorescence (especially during polluted, dusty or aged aerosol episodes)
Occupational, agricultural and source-oriented applications	WIBS	Detection of short-term source-related emissions and assessment of control measures or task-related exposure patterns in agricultural, composting/green-waste and embalming settings.	· Size and fluorescence filtering · Event-based analysis · Clustering and classification	Lack of standardized reference/ threshold values to comprehensively assess exposure
Fungal spore and pollen classification and monitoring	WIBS and Rapid-E(+)	Validated detection of fungal spore-related dynamics and supervised pollen classification using optical/UV-LIF measurements, with strongest pollen-classification evidence for Rapid-E(+) under representative and independently checked training/validation datasets.	Variety of approaches: - simple filtering based on size and fluorescence - clustering (typical of WIBS) - advanced supervised machine learning (CNN/ResNet) utilizing data relating to scattering, spectra and lifetime for Rapid-E(+)	Species-level attribution remains limited without: - microscopy, molecular markers, culture-based methods - advanced data analysis based on machine learning algorithms - other independent validation

reported in the text or tables of original articles) are provided in the Supplementary Materials [SM6-9]. In general, despite large differences in concentration levels, common patterns emerged, including diurnal cycles with peaks during nighttime and strong influence of meteorological conditions such as relative humidity, wind speed, and temperature. Interferents can affect the results, like long-range transport events, dust intrusions and local sources which further contribute to shaping the abundance and characteristics of fluorescent particles.

a. Urban sites

A total of 15 studies were focused on urban sites. Most of them were conducted in Asia (n = 9), followed by Europe (n = 5) and only one was carried out in America. An overview of fluorescent particles characteristics is provided in Table SM6.

Generally, FAPs exhibited a wide variability in concentrations across the studies (Calvo et al., 2018; Cheng et al., 2020; Gabey et al., 2011; Liang et al., 2024; Morrison et al., 2020; Sarangi et al., 2022; Yue et al., 2017, 2022), with average or median values ranging from 44 particles/L up to 5000 particles/L (measured in Spain by Calvo and colleagues (Calvo et al., 2018) and in Puerto Rico by Sarangi and colleagues (Sarangi et al., 2022), respectively), with intermediate levels of 990 particles/L and 1400 particles/L observed in China and Singapore by Yue and colleagues (Yue et al., 2022) and Li and colleagues (2020) (Morrison et al., 2020), respectively. Intra-study variability was also observed under different environmental conditions. Yu and colleagues (Yue et al., 2017) measured 642 particles/L during clean winter periods in China, with peaks up to 15,300 particles/L during polluted episodes, although the authors attributed this sharp increase to the presence of interferents such as PAHs, soil dust, biomass burning related particles. Liang and colleagues (Liang et al., 2024) reported an average concentration of 340 particles/L during spring 2021 in China, ranging from 780 particles/L in March (characterized by haze and dust events) to 330 and 290 particles/L in April and May, respectively. Gabey and colleagues (Gabey et al., 2011) and Cheng and colleagues (Cheng et al., 2020) reported FAP concentrations according to the three WIBS detection channel (FL1, FL2, FL3) measured in UK and China, observing comparable levels on the order of few hundred particles per Liter. Clancy and colleagues (Clancy et al., 2025) measured a total of 47.3 million in Dublin over a 40-day campaign (August-September 2019), of which 14% were classified as fluorescence (i.e., ~7.1 million particles), mainly of type B (43%, i.e., 3.05 million particles), BC (15% - i.e., 1.06 million particles) and ABC (14% - i.e., 0.99 million particles). Ma and colleagues (Ma et al., 2019) discriminated biological from non-biological fluorescent particles through cluster analysis, reporting total bioaerosol concentrations below 100 particles/L. Li and colleagues (Li et al., 2022) provided mass concentration of bioaerosol-like particles (classified according to rules in Table 2), assuming spherical shape and a density of 1.67 g/cm^3. FBAPs exhibited mass concentrations of 3.5 μg/m^3 during daytime, and 6.7 μg/m^3 during nighttime. Similarly, bacteria-like, fungi-like, and pollen-like particles also showed higher concentrations during nighttime (119.4 μg/m^3, 1.3 μg/m^3, and 51.6 μg/m^3, respectively) than during daytime (102.0 μg/m^3, 0.8 μg/m^3, and 26.3 μg/m^3, respectively).

This diurnal pattern, characterized by higher concentrations at night, is consistent with findings from other studies (Calvo et al., 2018; Fan et al., 2025; Ma et al., 2019; Sarangi et al., 2022) and partly agrees with Cheng and colleagues (Cheng et al., 2020) and Gabey and

colleagues (Gabey et al., 2011), who observed two daily peaks, at sunrise (~7:00 and ~9:00-10:00, respectively) and evening (both ~20:00), likely associated with fungal spores and bacteria. These peaks and higher concentrations of fluorescent particles were typically correlated with higher RH and lower wind speeds (Calvo et al., 2018; Cheng et al., 2020; Ma et al., 2019). Instead, concerning the influence of temperature, higher concentrations of bacteria and fungal spores were observed at lower temperatures, whereas pollen were associated with higher temperatures (Calvo et al., 2018; Cheng et al., 2020).

Beyond concentrations and their temporal trends, other studies focused on physical characteristics of fluorescent particles, particularly size and shape. O'Connor and colleagues (Oconnor et al., 2014) explored fluorescent particles in an urban area in Munich, reporting mean diameters of 8.0 μm for FAPs and 25.4 μm for "potential pollen" (i.e., fluorescent particles larger than 15 μm), with corresponding mean asymmetry factor (AF) values of 30.4 and 23.5. Fan and colleagues (Fan et al., 2025) and Clancy and colleagues (Clancy et al., 2025), observed FAPs mainly smaller than 8-10 μm, in Tianjin and Dublin, respectively. Consistently, Calvo and colleagues (Calvo et al., 2018) reported a Median Volumeter Diameter (MVD) of 11 μm. Therefore, comparable particle diameters were observed across studies, although it is worth noting the different metrics used. In contrast, Liang and colleagues (Liang et al., 2024) observed FBAPs in Beijing during spring to be mostly concentrated below 1 μm. Gabey and colleagues (Gabey et al., 2011) found size distributions with a primary mode at 1.2 μm and a secondary mode between 1.5 and 3 μm across all fluorescent channels. A bimodal size distribution was also observed by Yue and colleagues (Yue et al., 2017), with peaks between 2 and 5 μm, while Yu and colleagues (Yue et al., 2022) reported a single peak at 2.3 μm for all seven FAP types.

Environmental conditions appeared to significantly affect FAPs characteristics. During dust events, Liang and colleagues (Liang et al., 2024) observed that FAPs reached larger size ranges (with a size distribution peak at ~3 μm), while during clean and haze periods they remained consistently flatter. Moreover, during dusty period, AF sharply decreased from 28 to 14, suggesting altered particle morphology. Tang and colleagues (Tang et al., 2022) and Sarangi and colleagues (Sarangi et al., 2025) similarly investigated FAPs during aerosol and dust transport events, reporting increases in both concentration and fluorescence intensity, as well as changes in particle size and AF, highlighting the role of long-range transport in shaping the abundance and characteristics of fluorescent particles in urban environments.

b. Semi-urban/rural sites

Nine studies investigated bioaerosols in semi-urban sites, which were quite evenly distributed across Europe (n = 4), Asia (n = 3), and America (n = 2). An overview of fluorescent particles characteristics is provided in Table SM7.

Overall, slight lower concentrations were observed with respect to urban sites. Toprak and Schnaiter (2013a), O'Connor and colleagues (O'Connor et al., 2015a) and Morrison and colleagues (Morrison et al., 2020) measured fluorescent particles levels (either as total FAPs or considering each fluorescence channel) on the order of tens of particles per Liter [Table SM7]. In contrast, Addor and colleagues (Addor et al., 2022) measured a FAPs daily average of 390 particles/L while much higher concentrations were measured by Yu and colleagues (Yu et al., 2016), with average concentrations of 600 particles/L in FL1, 3400 particles/L in FL2 and 2100 particles/L in FL3, although the authors attributed these high levels to a large contribution from combustion-related aerosols, especially in FL1 channel.

The contribution of different FAPs types was explored in four studies (Addor et al., 2022; Markey et al., 2022; Negron et al., 2020; Yu et al., 2016). Different patterns were observed, but type B was found to be among the major contributors in all cases. In detail, the most abundant FAPs were: (i) B, ABC, and BC in Addor and colleagues' study (Addor et al., 2022); (ii) B, BC and C in and colleagues' study (Yu et al., 2016); (iii) AB and B in Markey and colleagues' study (Markey et al., 2022); A and B in Negron and colleagues' study (Negron et al., 2020).

As in urban sites, diurnal patterns of FAPs concentrations were observed. Generally, higher concentrations were recorded at night and minimum reached in the noon or early afternoon, and peaks in the early morning (Markey et al., 2022; O'Connor et al., 2015a; Toprak and Schnaiter, 2013a; Yu et al., 2016). Moreover, Toprak and Schnaiter (2013a) observed a seasonal cycle, with high FBAP number concentrations and fractions from late spring until early autumn, and the lowest concentration during winter. Average and median concentrations during each season are reported in Table SM7. Conversely, Morrison and colleagues (Morrison et al., 2020) measured lower concentration in August than September and October, when they peak, following a decrease and another peak at the beginning of November.

These last two studies found different correlations also between FAPs concentrations and weather conditions. More in detail, Toprak and Schnaiter (2013a) found correlation between FAPs concentrations and HR, while Morrison and colleagues (Morrison et al., 2020) observed that prolongated periods of low relative humidity were associated with exceptionally high bioaerosol concentrations (possibly indicative of spore showers). Moreover, Markey and colleagues (Markey et al., 2024) observed positive correlations between types A and B with rain and relative humidity, and negative correlation between FAPs greater than 5 μm and wind speed. The authors also assessed correlations between fluorescence particles and some pollutants, finding strong negative correlation between A and AB fluo-particles and most investigated pollutants, and strong association between B, and BC fluo-particles, especially with black carbon, NOx and NO_2 (with r values > 0.7).

The majority of FAPs fell within small particle size ranges. Xie and colleagues (Xie et al., 2017) observed a bimodal lognormal distribution in FL1, with the first peak at 1.35-1.5 μm and the second one occurring at 2.1-2.25 μm. Yu and colleagues (Yu et al., 2016) found that the highest FAPs number concentration came out at ~1 μm (except type ABC which peaked at 1–2 μm with and at 4–6 μm), and Addor and colleagues (Addor et al., 2022) found a hourly number-weighted mean diameters of 1.75 μm, with the highest peak occurring at 2.12 μm. O'Connor and colleagues (O'Connor et al., 2015a) observed median sizes of 4.5 μm in FL1 and 5.5 μm in FL2, and an interquartile range between 5 and 15 μm in FL3, while a median AF of 30 for total FAPs. Markey and colleagues (Markey et al., 2022) (Markey et al., 2022), explored the relationship between size and AF distributions, considering the prevalent (i.e., most abundant in the study) fluorescent fractions. According to the results, ABC type particles peaked at large size ranges, with a median AF value of 25, reasonably indicative of pollen-like particles. AB and A type particles resulted mostly in a diameter lower than 10 μm, with median AF values of 23 and 18, respectively, likely attributable to fungal spores.

c. Rural sites

Rural environments were the most investigated (n = 17), including forests, mountains, grasslands, marine areas and even the upper troposphere. Most of them were carried out in America (n = 7) and Europe (n = 6), followed by Asia (n = 3). One of them was performed in the Antarctic region. An overview of fluorescent particles characteristics is provided in Table SM8.

Gabey and colleagues (Gabey et al., 2010) and Whitehead and colleagues (Whitehead et al., 2010) investigated FAPs in tropical rainforest in Borneo, both above the canopy and understory. Lower concentrations were observed above the canopy (ranging between 50 and 300 particles/L) compared to the understory, where frequently exceeded 1500 particles/L. This level under the canopy is higher than average FAPs concentration of 400 particles/L observed by Whitehead and colleagues (Whitehead et al., 2016) in the Amazon rainforest at the ground level. Mountain areas generally exhibited low FAPs concentrations (Crawford et al., 2016; DeMott et al., 2025; Gabey et al., 2013). Average

concentrations on the order of a few ten of particles per Liter were measured by Gabey and colleagues (Gabey et al., 2013) and DeMott and colleagues (DeMott et al., 2025). Crawford and colleagues (Crawford et al., 2016) observed even lower FAPs concentrations, ranging from 0.27 particles/L during in-cloud periods to 6.3 particles/L during out-of-cloud periods; after applying a HACA, fluorescent particles of biological origin accounted for approximately 0.1 particles/L. Higher concentrations were reported by Yue and colleagues (Yue et al., 2019), who measured an average of 674 particles/L for total FAPs, with type B representing the most abundant fraction and suggesting a large contribute from non-biological sources. FL1 and FL3 channels accounted for mean concentrations of 190 and 281 particles/L, respectively, both greater but more consistent with the previous studies. Similarly, DeMott and colleagues (DeMott et al., 2025) found type B as the dominant class (63.2%), followed by type AB (16.0%) and A (12.5%).

Seasonal variations in FAPs types were observed by Shawon and colleagues (Shawon et al., 2025), with type A and C dominating during early summer (~60% and ~30%, respectively), and type C and B becoming prevalent from early August (~45% and ~24%, respectively). Comparable results were obtained by two studies performed in troposphere at high altitudes, aboard an aircraft (Perring et al., 2015, 2023). In the first study of Perring and colleagues (Perring et al., 2015), average FAP concentrations ranged between 21 and 87 particles/L, with elevated levels (~77 particles/L) observed in the marine boundary layer, possibly due to biomass emissions from warm marine environments. In Perring and colleagues (Perring et al., 2023), average concentrations were typically around 10 particles/L, although some flight levels showed values an order of magnitude lower. Such low concentrations are likely due to the absence of nearby sources of biological aerosols and anthropogenic interferents, as also observed by Moallemi and colleagues (Moallemi et al., 2021). In this study, FAPs concentrations were assessed along the Antarctic region aboard a research vessel, applying two detection thresholds for FAPs identification: 3σ and 9σ (referred to as fluorescent and hyper-fluorescent particles, respectively). Under pristine-marine conditions (i.e., uncontaminated or unaffected by anthropogenic activities or terrestrial sources), median concentrations of fluorescent and hyper-fluorescent particles were 11.4 and 0.87 particles/L, respectively, increasing to 17.3 and 1.52 particles/L in terrestrially influenced regions. Grassland areas were investigated by Tummon and colleagues (Tummon et al., 2024) and Forde and colleagues (Forde et al., 2019a). Tummon and colleagues (Tummon et al., 2024) focused only on pollen-like particles (defined by authors as ABC types greater than 20 μm), which showed average concentrations of ~0.05 particles/L. Instead, Forde and colleagues (Forde et al., 2019a) provided measurements carried out in 4 different monitoring campaigns, mainly grassland covered area (with different surrounding characterizes). All data were analysed through a HACA, and each cluster was associated to one or two types of bioaerosols or interferent type. Overall, most of the groups were attributed to the fungal spores, representing the main contributors in fluorescent particles, followed by bacterial and/or pollen fragments.

Focusing on diurnal cycle, FAPs concentrations were generally higher at night or in the early morning, while minimum levels were recorded in the afternoon. This diurnal pattern has been attributed to higher nocturnal RH and the breakup of the nocturnal boundary layer around sunrise (Crawford et al., 2014; Forde et al., 2019b; Gabey et al., 2010, 2013; Healy et al., 2014; Robinson et al., 2013; Shawon et al., 2025; Whitehead et al., 2016). However, some exceptions were reported. Yue and colleagues (Yue et al., 2019) measured higher concentrations of FAPs (747 particles/L) during daytime than night (458 particles/L), with a peak in the early afternoon and a minimum shortly before sunrise. Similarly, Gabey and colleagues (Gabey et al., 2010) recorded two peaks in the forest understory, one at midnight and the other one in the early afternoon. Shawon and colleagues (Shawon et al., 2025) did not observe any diurnal cycle at the beginning of the monitoring campaign (mid-June), but it became progressively more pronounced throughout the active grown seasons, reaching the strongest diurnal pattern in September for all types of FBAPs. However, different diurnal behaviours were observed for each fraction, with type A more abundant during night and early morning, and B, C and BC types showing increases after sunrise. The authors also noted that high concentration levels were not directly linked to precipitation, although higher precipitation rates corresponded with increased concentrations and more spherical and less rod particles shapes, possible due to the presence of more liquid water on the particles. Moreover, Gosselin and colleagues (Ila Gosselin et al., 2016) observed that ABC type (>65%) dominated the rainy periods, while BC and C types (>30% and >40%, respectively) dominated dry periods.

Differences in the size and shape of FAPs were found across the studies. A bimodal size distribution was observed by Gabey and colleagues (Gabey et al., 2010) in tropical rainforest, with two modes at 0.8–1.6 μm and at 2–3 μm (both above and under the canopy). Healy and colleagues (Healy et al., 2014) analysed size-distribution of FAPs measured at Killarney national Park, considering each fluorescence channel, observing a multimodal distribution in FL1 often dominated by smaller particles (<2 μm), a bimodal distribution with peak at ~1 μm and ~3 μm in FL2, and a much stronger signal at 3 μm for FL3. In contrast, Yue and colleagues (Yue et al., 2019) and Whitehead and colleagues (Whitehead et al., 2016) found monomodal distributions, with peaks at ~1 μm and ~1.8 μm, respectively. Perring and colleagues (Perring et al., 2015) reported that most FAPs in the Gulf region ranged between 1 and 4 μm. Conversely, O'Connor and colleagues (Oconnor et al., 2014) observed larger particle sizes, with average diameters of 7.6 μm and 26.6 μm for fluorescent particles and "potential pollen" (i.e., fluorescent particles >15 μm and with AF < 25, and high fluorescence in FL2 and FL3) at the Killarney National Park. Interesting outcomes were observed by Moallemi and colleagues (Moallemi et al., 2021), who observed differences between fluorescent and hyper-fluorescent particles. In detail, the size-resolved number concentration of fluorescent particles decreased continuously as particle diameter increased, while hyper-fluorescent particles showed a minimum at ~2 μm, followed by a peak at 5-8 μm. Moreover, the authors analysed the normalized PDFs (probability density functions) of single particle AF values segregated by size which revealed unimodal AF distributions with peaks at ~5 for particles smaller than 2.5 μm, and broader peaks ranging from 5 to 10 for particles between 2.5 and 5 μm and 10–20 for particles between 5 and 14 μm. Gabey and colleagues (Gabey et al., 2013) observed a bimodal distribution by plotting the asymmetry factor distributions (dN/dlogAF) of FAPs in the mountain region, with a primary mode at AF = 11 (during enhancements of concentrations), and a secondary broad mode at AF = 20. O'Connor and colleagues (Oconnor et al., 2014) reported mean AFs of 30.7 and 18.8 for fluorescent and potential pollen particles, respectively.

d. Occupational sites

Outdoor FAPs characterizing a composting/green waste facility, located in a remote rural area (approximately 6 km north of the Irish coastline) was investigated in two studies (Feeney et al., 2018; O'Connor et al., 2015b), considering different working periods across a week. An overview of fluorescent particles characteristics is provided in Table SM9. Generally, it was observed that different activities affect concentrations and characteristics of FAPs, although weather conditions also play an important role. In detail, O'Connor and colleagues (O'Connor et al., 2015b) distinguished three operational periods: (i) a "heavy workload" period (characterized by frequent deliveries and compost loading activities), (ii) "weekend" period, when the site was closed, and (iii) "light workload" period (with few deliveries and limited site activity). Higher FAPs were observed during the heavy workload period (average = 304.2 particles/L) compared to the light workload one (average = 109.9 particles/L). During the heavy workload period, maximum concentrations of fluorescent particles lower than 1.5 μm

occurred during working hours (between 08:00-15:00), showing a higher contribution than those during light workload period in increasing FAPs concentrations, when a maximum concentration occurred for a shorter time (at ~11 a.m.). However, the highest FAPs concentration was observed during the weekend, with an average of 320.2 particles/L, mainly due to a large contribution during nighttime hours, characterized by high relative humidity and low wind speed. Differences were observed also in particle size and shape across the periods. During the heavy and light workload periods, fluorescent particles were larger (average diameters of 1.8 μm and 2.1 μm, respectively) and more spherical/ellipsoidal (mean AF values of 26.7 and 24.2, respectively) compared to those observed during the weekend (average size = 1.2 μm; AF = 32.9).

Feeney and colleagues (Feeney et al., 2018) compare FAPs characteristics between weekday and weekend. A clear difference emerged between the two concentration profiles. The weekday period was dominated by compost site activities during working hours (9:00-17:00), with higher concentration of FAP, whereas the weekend appears to revert to a more rural profile in which fungal spores are mainly released at night, consistent with of O'Connor and colleagues (O'Connor et al., 2015b) outcomes. Notable, the authors did not record any striking relationships between FAPs concentrations and weather parameters (wind speed, temperature and relative humidity). The size distribution was consistent between weekday and weekend, with fluorescent particles displaying a bi-modal distribution, with most of the FAPs occurring <3 μm and two peaks at ~1.1 μm and ~2.1 μm.

3.4.2. Rapid-E instruments

A few studies (n° = 5) provided measurements performed outdoor through Rapid-E, all of them focused on the detection of large fluorescent particles, especially pollen grains. For Rapid-E(+), the contrast between threshold-based physical/fluorescence approaches and CNN-based pollen classification suggests that algorithmic treatment can be a primary determinant of performance, rather than a secondary post-processing step. High temporal resolution further allows the identification of short-lived pollen peaks, although scaling and validation against Hirst-type measurements remain a valuable support.

Morrison and colleagues (Morrison et al., 2020) investigated FPAs greater than 5 μm, between July and November 2018, in an urban environment in Hong Kong. As observed with the WIBS, concentrations were highly variable, but generally higher from October onwards. The lowest level was recorded in August, which increased in September and peaked at the start of October, followed by a decrease and by another increase at the beginning of November. Between 5th July and 1st October, the mean concentration of particles greater than 5 μm recorded by the PLAIR Rapid-E was 4.2 particles/L, while during periods of enhancement observed during October a peak up to 23 particles/L was recorded. Tummon and colleagues (Tummon et al., 2024) investigated pollen grains in a Swiss rural area and observed mean concentrations of 21 pollen grains/m^3 for daily, 6-h and hourly averages. Higher pollen concentrations were observed by Smith and colleagues (Smith et al., 2022) in an urban site in Croatia. The authors identified pollen through a CNN algorithm and reported a Seasonal Pollen Integral (SPIn) for total pollen of 29,502 pollen × day/m^3, over 242 days, meaning a daily average of ~122 pollen grains/m^3. SPIn for some pollen taxa during each specific pollen season were also investigated, and levels are reported in Table SM10. Daunys and colleagues (Daunys et al., 2021) aimed to find natural groupings of pollen by combing cluster analysis and neural networks classifications, based on a training dataset collected in lab. The authors investigated an urban environment in Lithuania and observed that most of fluorescent particles could be attributed to clusters including *Alnus*, *Artemisia*, *Betula*, *Festuca*, *Fraxinus*, *Pinus*, *Populus*, *Quercus*, *Salix*, *Secale*. Finally, González-Alonso and colleagues (González-Alonso et al., 2024) investigated the influence different meteorological on pollen measurements, observing positive correlations with temperature and relative humidity.

3.5. Comparisons with other instruments

In different studies UV-LIF instruments were co-located with other off-line instruments for the bioaerosols detection, and results were compared. Hereafter, the main outcomes were reported, mainly related to correlation and magnitude concentration levels similarity. Overall, comparisons with Hirst-type traps, microscopy, molecular tracers and flow cytometry indicate that UV-LIF instruments can capture temporal dynamics of selected bioaerosol classes, particularly fungal spores and pollen, but do not automatically provide taxonomic or viability-resolved identification. This is especially relevant for bacterial or low-nucleic-acid particle populations, which may be weakly or inconsistently detected by autofluorescence (Addor et al., 2023; Fernández-Rodríguez et al., 2018; Ila Gosselin et al., 2016; Negron et al., 2020; O'Connor et al., 2015a).

3.5.1. WIBS instruments

a. Comparisons with Hirs-type trap

WIBS data were compared to Hirst-type trap measurements in several studies, focusing both on fungal spores and pollen grains [Table SM11(a)]. As observed previously in outdoor studies, WIBS data were analysed in different ways (i.e., considering different fluorescent particles type, or classifying them into biological classes), and with different time resolutions.

Good correlations were found between total fluorescent particles and fungal spores at lower time-resolution, with a square correlation coefficient (R^2) ranging between 0.7 up to 0.9 for daily concentrations (Feeney et al., 2018; Fernández-Rodríguez et al., 2018; O'Connor et al., 2015a). Lower correlations were observed by Healy and colleagues (Healy et al., 2014), comparing fungal spores counts with the number concentrations from each WIBS fluorescent channel, with R^2 of 0.05, 0.29 and 0.38 for FL1, FL2 and FL3, respectively. Similar results were obtained from Clancy and colleagues (Clancy et al., 2025), in which weak Spearman's correlation coefficient ($\rho < 0.2$) was observed for most particle types fluorescing in FL1. However, it is interesting to report that the authors observed a bimodal distribution in the FL1 fluorescence intensities for ABC particles. After splitting ABC particles in two groups and adopting a fluorescence threshold of 9σ, the correlation with total spores increased in ABC_1 group, resulting in the highest correlation (R = 0.56), followed by BC (R = 0.53) and AC (R = 0.46) particle types. Analogous, Markey and colleagues (Markey et al., 2022) explored daily correlations between fungal spores and fluorescent particle types. Good correlations were observed with respect to A and AB types (R^2 ~0.65), negative correlations were found for B and BC types, and no significant correlations for C and ABC types. However, higher correlations were observed when considering A and B particles together, and particle A determined with a 9σ fluorescence threshold (R^2 = ~0.8). Regarding concentration levels, WIBS recorded higher particle number concentration (Feeney et al., 2018; Fernández-Rodríguez et al., 2018; O'Connor et al., 2015a), up to 200 times. However, despite differences in concentrations levels, it is interesting to note that O'Connor and colleagues (O'Connor et al., 2013) found correspondences in size and shapes of fungal spores sampled with the Hirst trap and fluorescent particles monitored with the WIBS.

Concerning comparisons with pollen grains, high correlations were found by O'Connor and colleagues (Oconnor et al., 2014) in the two measurement campaigns in Ireland (R^2 = 0.93) and Germany (R^2 = 0.98), considering fluorescent particles larger 15 μm. Instead, lower correlations were observed by Markey and collegues (Markey et al., 2022), considering the different fluorescent particle types, and Tummon and colleagues (Tummon et al., 2024), which focused only on ABC fluo-particles ≥20 μm, with r values ranging between ~0.2 and ~0.5. Moreover, Tummon and colleagues (Tummon et al., 2024) compared concentration levels and observed that WIBS provided almost

the half concentration than the two Hirst devices. Comparable concentrations were observed by Calvo and colleagues (Calvo et al., 2018) between BC and ABC particle types with an EOD (Equivalent Optical Diameter) greater than 2 μm and pollens. Quite low correlations were also observed by Clancy and colleagues (Clancy et al., 2025), with the highest correlation coefficient ($R = 0.52$) resulting from comparison with BC particle types (fluorescent threshold: 6σ) greater than 9 μm.

Differently from these studies, Markey and colleagues (Markey et al., 2022) performed some Multiple Linear Regression analysis between both fungal spores and pollen samples, weather parameters, and fluorescent particle types (FAP >2 μm for comparisons with fungal spores and FAP >8 μm for comparisons with pollen) detected with a WIBS4+. Overall, the highest R^2 (0.77) was observed between *Ascopores* and A and B particles (9σ), followed by the MLR (R^2 of 0.73) between tree pollen and DE particles (9σ). Herbs correlated quite well ($R^2 = 0.68$) with D and DE particles (9σ), *Cladosporium* and with ABC, BC and A (3σ; $R^2 = 0.66$) of 0.66, and *Poaceae* with D particles (9σ; $R^2 = 0.63$).

b. Comparisons with other instruments/approaches

Table SM11(b) summarizes studies that compared WIBS measurements with other techniques, different from Hirst-type trap.

Gabey and colleagues (Gabey et al., 2013) counted bacteria, yeast, fungal spores, pollen and plant debris through epifluorescence microscopy analysis, and compared the result with fluorescent particles data measured with a WIBS-3. In detail, four samples were collected through a cascade impactor sampler: one for 24 h (sample A), two exclusively during night-time (samples B and D), and one during daytime (sample C). Generally, a sort of correlation was found between the mean N_{NADH} ($\lambda_{excitation} \sim 300$ to 400 nm) and bacteria count, measured with WIBS and epifluorescence microscopy analysis respectively, with higher values on samples B and D, and both smallest during impactor C. However, for sample A, any link between measured bacteria concentration and observed N_{NADH} was recorded.

Yue and colleagues (Yue et al., 2019, 2022) explored the comparability of fluorescent data from a WIBS-4A with tracers for bioaerosols, identified through a fluorometer and UV-VIS spectrophotometer. Good correlations were observed between size-resolved mass concentration of FL1-FAPs (3σ and 6σ in the 2.5-10 μm), and both arabitol and mannitol, with R^2 ranging between 0.68 and 0.72 (Yue et al., 2019). Similar results were obtained by Gosselin and colleagues (Ila Gosselin et al., 2016), in which the authors compared fluorescence particles according to emission channel with arabitol, mannitol (1 → 3)-β-D-glucan and endotoxins during rainy and dry periods. According to results, R^2 ranged ~0.55-0.61 between fluorescence particles (FL, FL1, FL2, FL3) and arabitol during rainy periods, and an even stronger correlation ($R^2 > 0.81$) was observed between fluorescence particles and mannitol during rainy periods. Moreover, for the sake of completeness, high correlations were observed between fluorescence particles and CFU of fungal spores ($R^2 = \sim 0.54$ for FL1 and FL2; $R^2 = \sim 0.73$ for FL and FL3). Yue and colleagues (Yue et al., 2022) observed that type B, AB, BC, and ABC strongly correlate with the tracers of fungal spores and pollen (i.e., arabitol and sucrose, respectively), with a $R > 0.8$. The other types of FAPs, instead, moderately correlate ($0.5 < R < 0.8$) with fungal and pollen tracers. It is worth noting that the authors also investigated possible correlation with some possible interferences and observed that Ca^{2+} strongly or moderately correlates with a range of the coarse particles of all seven types of FAP, and that PAHs moderately correlate with particle types C, B, BC and ABC.

Negron and colleagues (Negron et al., 2020) compared flow cytometry analysis with WIBS-4A data, aiming to better understand the day-to-day variability of FBAPs. Among the outcomes, it is interesting to note that ABC-type is the only fluorescent particles type which showed a considerable correlation ($R^2 = 0.4$) with the high nucleic acid-content particles.

Finally, Addor and colleagues (Addor et al., 2023) compared WIBS-5/NEO data with (i) Optical Microscopy Counting (OMC), after sampling via an Allergenco-D spore trap, (ii) Microbial Cultivation (MC), after sampling through two-stage Andersen viable cascade impactors, and (iii) qPCR, after sampling with Button aerosol samplers. Spearman's correlation results were report in a table in the original paper, and they were not consistent between WIBS and the different traditional off-line methods. Especially, no significant correlations were found between fungi detected using OMC (Allergenco-D samples) and any of WIBS FAP types, except ABC outdoor which shown a negative correlation. Instead, through the MC, positive correlations were observed for indoor fungi and TFAPs >2 μm ($R = 0.75$), indoor bacteria and TFAPs ($R = 0.71$), and outdoor bacteria with TFAPs ($R = 0.61$), TFAPs >2 μm ($R = 0.75$) and FAP type AC ($R = 0.79$). Finally, through the qPCR analysis it was found that indoor fungi correlated with TFPAs >2 μm ($R = 0.47$), FAP type AB (0.64) and FAP type AC (0.39), bacteria indoor correlated with FAP types AB ($R = 0.42$) and AC ($R = 0.41$), and bacteria outdoors correlated with FAP type A (0.47). All correlations results are reported in a table in the original paper.

Overall, the comparison of WIBS measurements with traditional offline techniques have shown the potential of these instruments as a reliable proxy for bioaerosol temporal dynamics, especially at lower temporal resolutions. Strong correlations with Hirst-type trap were observed for both fungal spores and pollen, although notable discrepancies in concentration levels. Evidence indicates that the degree of agreement between methodologies is strongly influenced by the data processing approach rather than raw particle detection alone. Strategies such as size-selective filtering, the adoption of higher fluorescence intensity thresholds for the WIBS, and targeted grouping of particle types (e.g., types A and B for spores) have been consistently shown to enhance correlation with traditional methods. Moreover, comparisons with chemical tracers (e.g., arabitol and mannitol) further support the biological origin of specific fluorescent populations.

3.5.2. Rapid-E instruments

A few studies (n = 4) evaluated correlations between different pollens sampled with Hirst-type traps and identified through Rapid-E(+) instruments [Table SM12].

Tummon and colleagues (Tummon et al., 2024) classified pollen grains by adopting a physical and fluorescence-based approach. In detail the authors applied thresholds on particle size ("*which was estimated to be proportional to the square root of the total scattered light in the geometric regime*") and restricted the selection to particles with a bimodal-induced fluorescence spectrum, with thresholds on the intensity of the two modes and well-defined windows for their position. Number concentrations of pollen measured with two Hirst-type samplers were nearly 5 times higher than those detected by the Rapid-E, and correlations were quite low, with R values of ~0.20 for hourly averages and ~0.42 for daily averages. Differently, Smith and colleagues (Smith et al., 2022) identified pollen using a multi-input one-output CNN, trained on 23 different pollen types, and observed good correlations for hourly average concentrations of 7 pollens, with most of R values higher than 0.9. Matavuji and colleagues (Matavulj et al., 2022) evaluated different CNN-based classification models to identify pollens, which were alternatively trained and tested on two Rapid-E instruments, one in Novi Sad (Serbia) and the other in San Michele all'Adige (Italy). The authors observed stable correlations, even with uncertainty included (through Monte Carlo-based perturbation method). Overall, higher correlation coefficients for total pollen were observed between Rapid-E and Hirst-type trap measurements in Novi Sad (ranging between 0.73 and 0.85) than in San Michele all'Adige (ranging between 0.42 and 0.46). Finally, Sikoparija and colleagues (Sikoparija et al., 2024) adopted a ResNet architecture to classify fluorescent particles into fungal spores and pollen (as presented in paragraph 3.2.2.), detected with the Rapid-E+ operating in pollen mode. The authors found that Rapid-E+ recorded concentration an order of magnitude lower for both pollen and fungal spores, and the correlation coefficients of daily average

concentrations were 0.583 and 0.180 for total pollen and fungal spores, respectively. Correlation coefficients for each of the 23 fungal spore and pollen species are listed in the original paper.

4. Discussion

A total of 76 original articles met the inclusion criteria and were analysed in this systematic review. These corresponded to 79 instrument-specific study records because three studies investigated both WIBS and Rapid-E(+). The revised synthesis highlights that instrument type, operational mode and data-treatment strategy are inseparable determinants of reported performance. Overall, the studies demonstrated substantial heterogeneity in terms of research objectives, instrumentation models and versions, data analyses and investigated environments. This variability occasionally complicated direct comparisons across studies, limiting the ability to derive generalizable conclusions, despite all works share a common underlying focus: the investigation of biological aerosols, using the fluorescent particles as a proxy, through UV-LIF-based instruments that allow for continuous, real-time monitoring. A first difference lies in the structural and functional characteristics between WIBS and Rapid-E(+) instruments which, although based on the same approach, detect and analyse the fluorescence response of particles differently, as described in the introduction and presented in Table SM1 and Table SM2. Also, these instruments have different nominal optical size ranges, broader for the Rapid-E(+) (0.5-100 μm for Rapid-E, and 0.3-100 μm for the Rapid-E+) than for the WIBS (ranging between 0.5 or 0.8 up to 20 or 30 μm). This may partly explain the outcomes from laboratory studies assessing counting performance of total and fluorescent particles, with WIBS instruments showing better detection of finer particles (especially in the range 1-2 μm) than Rapid-E(+) which has shown better performance for the larger ones (mainly around 10 μm). Another possible reason can lie in the different flow rates (i.e., 5.0 L/min for the Rapid-E(+), ~0.3 L/min for the WIBS) which can lead to an under- or over-counting of particles (Heim et al., 2008). Consequently, the fluorescence particle count can be affected by a certain degree of uncertainty, also considering that the analysis requires more time (although it is only few nanoseconds) than the mere detection of particles. Moreover, another relevant aspect concerns the *intra*-model variability across the various versions, with the most recent typically characterized by larger detection size range and the intrinsic improvements introduced through hardware and software updates. Related to this, a lack of clarity sometimes emerged from the studies, as when no clear specifications of the operational mode, fluorescence threshold and pre-processing of data are provided in the study designs, highlighting the absence of standardized procedures for the monitoring, possibly according to the investigated environment and the aims. However, it should be noted that these instruments are quite recent and constantly evolving, therefore it is not always straightforward to determine the best approach. For example, concerning the WIBS, a 3σ fluorescence threshold is recommend by the manufacturer, but as emerged from some studies, this can be too low and does not always allow to exclude interferents. On the other hand, a higher fluorescence threshold (e.g., 6σ or 9σ) may does not allow for the detection of biological aerosols with a low fluorescence intensity, bringing to underestimations of concentration. A sort of trade-off can be found by adopting grouping and classification of fluorescent particles into biological agents and interferents, which resulted be effective in discriminating between true and false positives (i.e., biological agents and fluorescent interferents), but more challenging in the proper classification of different bioaerosol types. Generally, these approaches can be structured at multiple levels and vary in complexity, as well as in their resource and time requirements. Concerning the WIBS, fluorescent particles can be classified according to the emission channel (i.e., FL1, FL2, FL3) and their combinations (i.e., types A, B, C, AB, AC, BC, ABC), providing a first overview and interpretations. For example, the literature identified A type particles as the common fingerprint of bacteria, while FL2 and B type particles were often related to interferences, allowing authors for a first discrimination. Multivariate data analysis can provide a further step on discrimination, although some input and output parameters need to be defined (e.g., linkage criteria, distance metric, the final number of clusters), slightly increasing the complexity of analysis and making it more study-specific and related to the interpretation of authors. To better explain this point, a cluster resulting from the analysis displays some average values of the variables selected, as for the size, shape and fluorescence emission characteristics. Based on this information, authors can interpret the clusters and classify them as bacteria-like or fungi-like, although distinctions among biological agents are not always clear, making accurate classification challenging. Some clustering approaches were explored from few studies, with HACA providing the best results, followed by DBSCAN and k-means, while gradient boosting yielded poor performance. Alternative approaches are instead suitable for the Rapid-E(+) due to the instrument design and nature of data. As emerged from the literature, data analysis mainly relies on ML algorithms, especially models based on neural networks (like ANN and CNN), which are trained on a reference dataset (more properly called "training dataset") making them very specific and reliable for the reference species, thus allowing for a more in-depth level of exploration. It is interesting to note that these studies involved mainly pollen and fungal spores, while no studies were conducted on bacteria. Despite this, which may reduce the consideration to two classes of bioaerosols, extremely high performances in discrimination across different species were observed, especially by implementing more input data or, concerning the Rapid-E+, selecting the proper operational mode. However, these approaches are time and resource-consuming, and the gain in performance is not linear, leading to a trade-off between model complexity, achievable accuracy, and computation time. Moreover, it emerged that these models can be implemented on the same instrument used to build the training dataset, making them non-transferable, although evidence indicates that better performance can be achieved by training models adding missing information (i.e., bioaerosols species) from an external training database. In order to provide a schematic overview, Table 4 summarizes the main data-treatment approaches identified in the reviewed studies, indicating their typical application domains, strengths, limitations and the validation requirements needed to support biological interpretation.

This heterogeneity in data analysis is then observed in studies performed in different settings. Clearly, part of the variability is since each of them is characterized by different aims which primarily guide the study design. However, for the same goal different data analysis can be adopted and the outcomes are not presented in a consistent way. As observed, a few studies were conducted indoors, all of them through WIBS instruments. Generally, higher concentrations of FAPs were observed related to occupancy periods, despite the time resolution adopted for the analysis (i.e., by comparing working with non-working hours or days), as emerged from monitoring campaign conducted inside office and residential environments, and also from monitoring in a subway station (in which higher occurred during rush hours). A notable outcome, in contrast with the others, emerged from Lancia and colleagues (Lancia et al., 2023) where no clear differences in bacteria-like particle concentrations emerged between working and non-working days. This can be due to the lower time resolution, which considered both working and non-working hours for the working days, or to the slight differences in the classification criteria with respect to others, also since fungal- and pollen-like particles displayed increases during working-days. In one hand, this can point out the role and the impact of different criteria and data analysis, although in the other hand this does not mean that with different classification rules higher bacteria would have been observed. Increases in FAPs concentrations were also recorded during specific activities in three thanatopraxy laboratories, highlighting the utility of these instruments for identifying exposure risk scenarios and supporting appropriate risk management strategies. Spatial and temporal patterns according to different background

Table 4
Data-treatment approaches and validation requirements in WIBS and Rapid-E(+) studies.

Data-treatment approach	Instrument(s)	Typical use in included studies	Contribution to interpretation	Main caveat and validation needs
Fluorescence thresholding	WIBS and Rapid-E(+)	Initial identification of fluorescent particles and estimation of FAP/FBAP concentrations	Transparent and reproducible when thresholds and background procedures are reported	Threshold choice strongly affects fluorescent fractions and sensitivity to weakly fluorescent particles or interferents
Conservative threshold strategies (e.g. 9σ)	Mostly WIBS	Reduction of weakly fluorescent non-biological interferents in complex or polluted environments	Improves specificity for strongly fluorescent particles and helps control dust/combustion-related interference	May remove weakly fluorescent biological particles and reduce sensitivity
Size- and channel-based filtering	Mostly WIBS	Target-specific selection of pollen-size particles, fungal-spore-like particles or protein-like fluorescence categories	Can improve agreement with Hirst, microscopy, chemical tracers or source-related expectations	Relies on assumptions about target particle size/channel behaviour and may exclude relevant fragments or aged particles
Hierarchical and partition-based clustering (e.g., agglomerative, k-means, DBSCAN)	Mostly WIBS	Exploratory separation of particle populations using size, fluorescence intensity and asymmetry/scattering features	Useful for identifying recurring fluorescent particle classes and source/event-related patterns without prior labelling	Sensitive to normalization, distance metrics, and algorithm parameters (e.g., number of clusters, epsilon); cluster interpretation remains subjective
Classical supervised machine learning (e.g., Random Forest, SVM, Gradient Boosting)	Mostly WIBS	Supervised classification of particles using labelled laboratory references or well-characterized ambient datasets	Outperforms simple clustering and thresholding where reliable reference libraries exist, allowing for robust particle identification	Model generalizability relies heavily on training-set representativeness; transparent feature reporting and cross-validation remain critical
CNN, ResNet and related deep-learning architectures	Rapid-E(+)	Classification of pollen and fungal spores from scattering, fluorescence spectra and lifetime data	Can exploit multimodal particle-level information and improve classification performance in labelled datasets	Strong dependence on training-set representativeness, reference labels, device-specific response and transferability
Vision Transformer/ computer-vision approaches	Rapid-E(+)	Exploratory use of computer-vision models on scattering-image data	Potentially useful for extracting information from scattering patterns beyond handcrafted features	Direct evidence for routine application to WIBS/Rapid-E(+) bioaerosol monitoring remains limited
Hybrid UV-LIF and offline validation	WIBS and Rapid-E(+)	Combination of high-time-resolution fluorescent particle data with microscopy, tracers, culture, flow cytometry, qPCR/dPCR, sequencing or others	Links short-term dynamics with biological, chemical or taxonomic interpretation	Requires coordinated sampling and careful temporal alignment between real-time and offline methods
Sensor-fusion/contextual interpretation	Primarily WIBS, applicable to Rapid-E(+)	Integration of UV-LIF features with PM size distributions, BC/EC, chemistry, meteorology, source-receptor or trajectory analysis	Improves interpretation in complex environments affected by pollution, dust, rain, biomass burning or transport	Does not by itself provide taxonomic attribution; still requires biological validation where needed

conditions were observed also outdoors. Most of the measurements were conducted with the WIBS, but as outlined before there was considerable variability among the study designs, with differences concerning the type of investigated environment (urban, semi-urban/rural, rural, occupational), period and duration of the monitoring (like few days during a season to continuous monitoring for a whole year), versions of instruments which can have by different operational modes, and approach to data analyses. Despite all these aspects making data not so immediately comparable, some consistent results and outcomes emerged across them. Firstly, higher FAPs concentrations were observed in urban, semi-urban/rural and forest environments (typically ranging in the order of hundreds or few thousands of particles per liter) than remote rural locations (usually in the order of few tens particles per liter), highlighting the role of both biological and anthropogenic aerosols sources. However, in urban environments, type B fluorescent particles were often among the most contributors, generally associated with anthropogenic interferences, thus explaining the greatly observed levels. Moreover, it is interesting to note that large fractions of type B particles were also observed in mountain areas, considered by the authors to have a strong anthropogenic contribution in this case as well, despite the remote locations. This result interpretation is based on evidence from laboratories studies, in which it was seen that non-biological particles can emit fluorescence detected on FL2, highlighting the potential of LIF-based instruments in detecting long range transport of some airborne pollutants, which can affect air quality of remote locations, such as mountains (Arellano et al., 2011; Wei et al., 2024). However, a certain degree of caution in this interpretation should be required as some bacteria and fungal spores can emit in FL2, therefore proper and careful analysis is important. Clear and consistent outcomes emerged for the diurnal cycle and weather influence. Despite some exception, most of the studies found higher concentrations at higher RH, explaining higher levels recorded during nights (when RH increases), and low wind speed. The role of weather conditions clearly emerged in the occupational studies in O'Connor et al., 2015 (O'Connor et al., 2015c), which can be more relevant than performed activities, with the weekend providing higher concentration than weekdays, in contrast with the other study. On the other hand, less clear outcomes emerged for the annual and seasonal temporal trends. Only a study (Toprak and Schnaiter, 2013b) provided FPAs concentrations across all four seasons, finding higher concentrations during summer than winter. But inconsistent results also emerged, with some studies performed during winter showing higher concentrations, others lower, and the same is for studies performed during spring and summer. As mentioned at the beginning of this paragraph, it is not always easy to compare data, due to the large variability and a lot of factors that can affect the concentration (location and sources, weather conditions, etc.). Likely for the different study designs, no clear outcomes emerged also from analysis of size and shapes. This information can provide important characteristics of bioaerosols, but they look more study-specific, according to local environmental characteristics. Outdoor studies performed with Rapid-E(+) instruments were mainly focused on pollen grains or particles greater than 5 μm, likely agree and partly reflect the better ability and exploitability of Rapid-E(+) in detecting larger particles, as emerged from laboratory studies. In one study, higher pollen concentrations were observed under conditions of increased temperature and relative humidity, highlighting the relevance of meteorological variables as observed in WIBS studies. Another study reported higher concentrations of fluorescent particles larger than 5 μm during the autumn period compared with summer. However, this finding contrasts with the previous since summer is typically characterized by higher levels of RH and temperature. Overall, given the limited number of studies investigating the use of the Rapid-E(+) in outdoor environments, it remains challenging to identify consistent trends or draw general conclusions. Nevertheless, the available studies may serve as a valuable reference for

Table 5
Minimum reporting items for UV-LIF-based bioaerosol studies.

Domain	Minimum reporting item	Why it should be reported
Instrument and configuration	· instrument model/version (e.g. WIBS-4A, WIBS-NEO, WIBS-4+, Rapid-E or Rapid-E+) · Manufacturer · firmware/software · operating mode and gain settings	Instrument versions and detector settings affect size and fluorescence response and comparability across studies
Sampling design	· sampling site · inlet height · flow rate · sampling duration · temporal resolution/aggregation · indoor/outdoor configuration	Sampling geometry and aggregation determine representativeness and comparability, and allow for results interpretation across studies
Particle sizing	· effective particle size range · excluded size fractions · size calibration	Size response differs across instruments and affects assessment and interpretation of particles concentrations, bacteria, spores, pollen, fragments and non-biological interferents, as well
Fluorescence threshold	· fluorescence threshold adopted (e.g., baseline + 3σ for WIBS, or specific lifetime/scatter gating for Rapid-E) · forced-trigger/background procedure	Threshold choice strongly affects fluorescent fraction, particle-type classification and false-positive control
Calibration and reference materials	· sizing and fluorescence calibration materials (e.g., PSL/fluorescent bead standards or fluorophore-equivalent) · frequency of calibration and any normalized/intensity-calibrated reporting	Calibration is essential for inter-study and inter-instrument comparison, particularly when using fluorescence intensity features
Pre-processing and quality control	· particle filtering · missing-particle correction · background subtraction · normalization, transformations and exclusion criteria	Pre-processing decisions can change any outcomes related to concentrations, classification and analysis, and performance metrics
Classification algorithm	· threshold/filtering rules · classification/clustering algorithm, its architecture and parameters · software/code/packages availability and versions	Algorithmic treatment is a primary determinant of performance, especially for Rapid-E(+) classification
Training and validation	· training dataset · reference labels · independent validation dataset · cross-validation design · cross-site/device transferability	Performance may not transfer across devices, sites or reference datasets without validation
Reference/offline methods	· Hirst/microscopy, culture, qPCR/dPCR, sequencing, flow cytometry, chemical tracers · other reference/offline methods · comparison metric	Independent methods are required for taxonomic, viability-related or biological attribution beyond fluorescent proxies
Environmental and co-pollutant context	· meteorology · land use · dust and pollution episodes or similar · trajectory/source-receptor analysis	Contextual variables help distinguish biological emissions from fluorescent interferents and transported events
Uncertainty and interpretation limits	· false positives/negatives · instrument limitations · biological attribution level (i.e., whether results are interpreted as FAP/PBAP proxies, taxonomic classes or validated biological categories) · uncertainty in concentration and comparability	Prevents over-interpretation of UV-LIF signals as direct taxonomic or viability-resolved measurements

future research, guiding further investigations aimed at expanding current knowledge in this field. The validity of measurements obtained from these two instruments has been investigated in several studies through comparisons with traditional or alternative measurement techniques. Most of these studies relied on comparisons with the Hirst-type trap, which represents the regulatory reference method; however, this approach does not allow for the sampling and identification of bacteria. With regard to WIBS measurements, good correlations have been reported between fungal spore and pollen sampling and fluorescent particle counts, whereas more inconsistent results have been observed for the classification into specific biological agents. In particular, for fungal spores, especially at high temporal resolution, correlations tend to be lower, while for pollen even relatively simple size-based classification approaches have yielded improved agreement. For the Rapid-E(+), simpler physical- and fluorescence-based approaches did not result in satisfactory correlations, whereas improved performance was observed when particle classification was conducted using neural network models. In both cases, however, the Hirst-type sampler generally provided higher concentration values than both the WIBS and the Rapid-E(+), with larger discrepancies reported for the latter. WIBS measurements have also been compared with other approaches, including fluorescence-based methods focusing on biological tracers (such as mannitol and arabitol), as well as with bacterial plate counts, which cannot be assessed using Hirst-type traps. Overall, the reported results are somewhat heterogeneous, with correlations that are at times higher and at times lower, likely reflecting a combination of factors related both to the intrinsic characteristics of the measurement techniques and to the data processing strategies applied. Recent Rapid-E(+) studies indicate that deep-learning approaches, particularly CNN-based architectures, can improve classification performance compared with simpler threshold-based or purely physical/fluorescence approaches. To complement the qualitative synthesis, Table SM13 provides a structured semi-quantitative overview of selected key performance-related indicators reported across laboratory and field studies. These include counting efficiency, classification accuracy, precision/recall/F1-score, and correlations or agreement metrics with reference/offline methods, while acknowledging that differences in study design, instruments, targets and data-treatment approaches limit direct comparability.

In particular, multi-input CNNs and residual architectures have been used to combine scattering patterns, fluorescence spectra and fluorescence lifetime data, with performance gains reported after hyperparameter tuning and architecture/training-strategy optimization

(Boldeanu et al., 2022; Brdar et al., 2023; Bruffaerts et al., 2025; Matavulj et al., 2022, 2023; Šauliene et al., 2019). However, these models are highly dependent on the representativeness of training datasets, instrument-specific responses and validation against independent reference methods, as shown by the drop in performance observed when models trained on one Rapid-E(+) device or reference dataset were applied to another device or location (Matavulj et al., 2022; Sikoparija et al., 2024). Vision Transformer-based computer-vision models have recently been explored for Rapid-E scattering data, and the availability of high-frequency UV-LIF/Rapid-E time series makes event-oriented or sequence-aware modelling conceptually relevant. Nevertheless, direct evidence for the routine application of Transformer-based or other sequence-learning architectures to WIBS/-Rapid-E(+) bioaerosol datasets remains limited (Daunys et al., 2024; Smith et al., 2022). As previously observed in Table 4, a recurrent methodological heterogeneity can be found in the included studies. Table 5 summarizes a set of minimum reporting items that should be considered when presenting UV-LIF bioaerosol measurements, in order to improve reproducibility, comparability and interpretation across instruments and study settings. These include instrument version, operating mode, flow rate, effective particle size range, fluorescence threshold, forced-trigger/background correction procedure, detector settings, calibration materials, pre-processing steps, classification algorithm, training and validation datasets, reference/offline methods, temporal aggregation, meteorological context, co-pollutants and uncertainty sources. Also, because the interpretation of UV-LIF data depends strongly on pre-processing, classification strategy and independent validation, Figure SM1 provides a conceptual pipeline summarizing the main steps from particle-level optical detection and fluorescence analysis to biological attribution in WIBS and Rapid-E(+) studies.

At the current state of the art, UV-LIF instruments should not be considered absolute substitutes for taxonomic or viability-resolved methods, because fluorescence-based signals generally provide proxy information on fluorescent aerosol particles rather than direct biological identification, viability assessment or species-level attribution (Fennelly et al., 2017; Negron et al., 2020; Savage et al., 2017). Rather, they can complement offline methods by acting as high-time-resolution sentinels for short-term fluorescent particle events, temporal patterns and emission episodes that would otherwise be poorly resolved (O'Connor et al., 2015b; Smith et al., 2022; Tang et al., 2022). In this hybrid framework, periods characterized by UV-LIF peaks can be prioritized for microscopy, culture-based analysis, chemical tracer measurements, qPCR/dPCR or sequencing-based confirmation, thereby linking real-time dynamics with biological attribution (Ila Gosselin et al., 2016; Negron et al., 2020; Santander et al., 2021). In addition, atmospheric aging represents a major challenge for UV-LIF-based biological attribution. Exposure to oxidants, photochemical processing and interactions with secondary organic aerosol can modify the intensity and spectral properties of biological particles, while non-biological fluorescent particles such as SOA, HULIS, PAHs, soot and mineral dust can mimic biological fluorescence. Therefore, classification models trained only on fresh laboratory-generated bioaerosols may not be fully transferable to polluted or atmospherically aged outdoor environments. Future training datasets should include aged biological particles and environmentally relevant non-biological interferents (Ackerman et al., 2025; Cheng et al., 2020; Liang et al., 2024; Markey et al., 2022; Savage et al., 2017). Multi-sensor data fusion is a promising strategy to improve the interpretation of UV-LIF measurements in complex environments, where fluorescent particle signals are shaped by biological emissions, meteorology, transport and anthropogenic pollution. Combining UV-LIF particle-level information with PM size distributions, black carbon/elemental carbon or other combustion proxies, meteorological variables, chemical tracers and offline biological measurements may help distinguish biological sources from non-biological fluorescent interferents, particularly during urban pollution, haze, biomass-burning or dust events (Cheng et al., 2020; Forde et al., 2019a; Liang et al., 2024; Markey et al., 2024; Negron et al., 2020; Savage et al., 2017). Taken together, these findings suggest that both the WIBS and the Rapid-E(+) are generally capable of capturing variability associated with bioaerosol concentrations, although some limitations have been reported with respect to the absolute order of magnitude of the measured values. With regard to the classification of fluorescent particles into biological classes, the WIBS appears to exhibit greater limitations compared with the Rapid-E(+), whose classifications are based on neural network approaches. This comparison highlights two complementary aspects: on the one hand, more complex approaches can provide more robust and detailed results, but are time and resource intensive and require a higher level of expertise; on the other hand, simpler approaches allow for more immediate analyses and interpretations, which are generally robust when considering fluorescent particle counts, but still require further development and validation for more detailed biological identification. In health-oriented applications, networked UV-LIF monitoring could support exposure assessment for allergic diseases and asthma-related studies by providing high-time-resolution information on pollen, fungal spores and sub-pollen/fluorescent particle events that are not captured by daily or delayed reference methods (Oconnor et al., 2014; Smith et al., 2022; Tešendić et al., 2020; Venkatesan et al., 2025). Similar approaches may also be useful for occupational and healthcare bioaerosol surveillance, where real-time instruments can identify short-term emission episodes during source-related activities or aerosol-generating procedures. In addition, continuous UV-LIF monitoring may contribute to early-warning frameworks for unusual fluorescent particle events associated with meteorological changes, precipitation, dust transport or pollution episodes (Liang et al., 2024; O'Connor et al., 2013, 2015b; Tang et al., 2022; Wingert et al., 2022). However, such applications require careful validation against biological endpoints, including microscopy, cultivation, molecular tracers, flow cytometry, qPCR/dPCR or sequencing, and, where public-health interpretation is intended, against epidemiological, symptom-based or clinical indicators (Ila Gosselin et al., 2016; Negron et al., 2020; Smith et al., 2022; Tešendić et al., 2020).

5. Conclusions

This systematic review shows that WIBS and Rapid-E(+) have substantially advanced real-time bioaerosol monitoring by enabling high-time-resolution detection of fluorescent aerosol particles across laboratory, indoor and outdoor settings. However, the reviewed evidence also shows that UV-LIF signals should be interpreted as bioaerosol proxies rather than direct taxonomic identification, unless supported by robust data treatment and independent validation. WIBS instruments appear particularly suitable for long-term FAP/PBAP monitoring, source/event tracking and indoor/outdoor temporal-pattern assessment, owing to their operational simplicity and established use in field studies. Rapid-E (+) provides richer spectral, lifetime and scattering information and is therefore especially promising for supervised classification tasks, such as pollen and fungal-spore discrimination, although its performance depends strongly on training datasets and model transferability. Across both platforms, comparability remains limited by heterogeneous thresholds, calibration strategies, pre-processing choices, operational modes, reference methods and reporting practices. For this reason, we propose a minimum reporting checklist and emphasize the need for harmonized calibration, validation and data-processing protocols.

Future applications should move toward hybrid monitoring frameworks in which UV-LIF instruments provide real-time detection of fluorescent particle events and trigger or complement offline confirmation by microscopy, culture-based methods, chemical tracers, qPCR/dPCR or sequencing. This integrated approach is particularly important in polluted urban atmospheres, haze or dust events, and health-oriented exposure assessment, where non-biological fluorescent interferents and atmospheric aging may affect biological attribution.

Funding

No funding was secured for this study.

CRediT authorship contribution statement

Alessio Carminati: Conceptualization, Investigation, Writing – original draft, Writing – review & editing. **Andrea Spinazzè:** Conceptualization, Investigation, Writing – original draft, Writing – review & editing. **Francesca Borghi:** Conceptualization, Investigation, Writing – original draft, Writing – review & editing. **Stefano Boscolo:** Writing – review & editing. **Giacomo Fanti:** Writing – review & editing. **Eleonora Pagani:** Writing – review & editing. **Carolina Zellino:** Writing – review & editing. **Andrea Cattaneo:** Supervision. **Domenico Maria Cavallo:** Supervision.

Declaration of competing interest

The authors declare that they have no known competing financial interests or personal relationships that could have appeared to influence the work reported in this paper.

Appendix A. Supplementary data

Supplementary data to this article can be found online at https://doi.org/10.1016/j.atmosenv.2026.122220.

Data availability

The main data supporting the findings of this study are available within the paper, its references, and Supplementary Material. Other data will be made available on request.

References

Ackerman, D.N., Pan, Y.-L., Kalume, A., Klug, E.A., Ravnholdt, A.R., Crown, K.K., et al., 2025. The impact of environmental aging processing on bioaerosol detection using circular intensity differential scattering (CIDS). J. Aerosol Sci. 186. https://doi.org/10.1016/j.jaerosci.2025.106555.

Addor, Y.S., Baumgardner, D., Hughes, D., Newman, N., Jandarov, R., Reponen, T., 2022. Assessing residential indoor and outdoor bioaerosol characteristics using the ultraviolet light-induced fluorescence-based wideband integrated bioaerosol sensor. Environ. Sci. Process. Impacts 24, 1790–1804. https://doi.org/10.1039/d2em00177b.

Addor, Y.S., Newman, N., Baumgardner, D., Indugula, R., Hughes, D., Jandarov, R., et al., 2023. Assessment of indoor bioaerosol exposure using direct-reading versus traditional methods—potential application to home health care. J. Occup. Environ. Hyg. 20, 401–413. https://doi.org/10.1080/15459624.2023.2212007.

Arellano, L., Fernández, P., Tatosova, J., Stuchlik, E., Grimalt, J.O., 2011. Long-Range transported atmospheric pollutants in snowpacks accumulated at different altitudes in the Tatra Mountains (Slovakia). Environ. Sci. Technol. 45, 9268–9275. https://doi.org/10.1021/es202111n.

Šauliene, I., Šukiene, L., Daunys, G., Valiulis, G., Vaitkevičius, L., Matavulj, P., et al., 2019. Automatic pollen recognition with the Rapid-E particle counter: the first-level procedure, experience and next steps. Atmos. Meas. Tech. 12, 3435–3452. https://doi.org/10.5194/amt-12-3435-2019.

Boldeanu, M., Burileanu, C., Cucu, H., Marmureanu, L., 2022. Pollen classification using classical ML algorithms on fluorescence and scattering data. Univ. Politeh. Buchar. Sci. Bull. Ser. C-Electr Eng. Comput. Sci. 84, 123–136.

Boldeanu, M., Cucu, H., Burileanu, C., Mărmureanu, L., 2021. Multi-input convolutional neural networks for automatic pollen classification. Appl Sci Switz 11. https://doi.org/10.3390/app112411707.

Brdar, S., Panić, M., Matavulj, P., Stanković, M., Bartolić, D., Šikoparija, B., 2023. Explainable AI for unveiling deep learning pollen classification model based on fusion of scattered light patterns and fluorescence spectroscopy. Sci. Rep. 13. https://doi.org/10.1038/s41598-023-30064-6.

Bruffaerts, N., Graf, E., Matavulj, P., Tiwari, A., Pyrri, I., Zeder, Y., et al., 2025. Advancing automated identification of airborne fungal spores: guidelines for cultivation and reference dataset creation. Aerobiologia 41, 505–525. https://doi.org/10.1007/s10453-025-09864-y.

Calvo, A.I., Baumgardner, D., Castro, A., Fernández-González, D., Vega-Maray, A.M., Valencia-Barrera, R.M., et al., 2018. Daily behavior of urban fluorescing aerosol particles in northwest Spain. Atmos. Environ. 184, 262–277. https://doi.org/10.1016/j.atmosenv.2018.04.027.

Cheng, B., Yue, S., Hu, W., Ren, L., Deng, J., Wu, L., et al., 2020. Summertime fluorescent bioaerosol particles in the coastal megacity Tianjin, North China. Sci. Total Environ. 723. https://doi.org/10.1016/j.scitotenv.2020.137966.

Clancy, J.H., Markey, E., Martínez-Bracero, M., Maya-Manzano, J.M., McGillicuddy, E.J., Sewell, G., et al., 2025. Comparative analysis of real-time fluorescence-based spectroscopic instruments: bioaerosol detection in the urban environment of Dublin City, Ireland. Atmosphere 16. https://doi.org/10.3390/atmos16030275.

Crawford, I., Lloyd, G., Herrmann, E., Hoyle, C.R., Bower, K.N., Connolly, P.J., et al., 2016. Observations of fluorescent aerosol-cloud interactions in the free troposphere at the high-altitude research station jungfraujoch. Atmos. Chem. Phys. 16, 2273–2284. https://doi.org/10.5194/acp-16-2273-2016.

Crawford, I., Robinson, N.H., Flynn, M.J., Foot, V.E., Gallagher, M.W., Huffman, J.A., et al., 2014. Characterisation of bioaerosol emissions from a Colorado pine forest: results from the beachon-rombas experiment. Atmos. Chem. Phys. 14, 8559–8578. https://doi.org/10.5194/acp-14-8559-2014.

Crawford, I., Ruske, S., Topping, D.O., Gallagher, M.W., 2015. Evaluation of hierarchical agglomerative cluster analysis methods for discrimination of primary biological aerosol. Atmos. Meas. Tech. 8, 4979–4991. https://doi.org/10.5194/amt-8-4979-2015.

Daunys, G., Šukienė, L., Vaitkevičius, L., Valiulis, G., Sofiev, M., Šaulienė, I., 2021. Clustering approach for the analysis of the fluorescent bioaerosol collected by an automatic detector. PLoS One 16. https://doi.org/10.1371/journal.pone.0247284.

Daunys, G., Šukienė, L., Vaitkevičius, L., Valiulis, G., Sofiev, M., Šaulienė, I., 2024. Comparison of computer vision models in application to pollen classification using light scattering. Aerobiologia 40, 109–121. https://doi.org/10.1007/s10453-022-09769-0.

DeMott, P.J., Mirrielees, J.A., Petters, S.S., Cziczo, D.J., Petters, M.D., Bingemer, H.G., et al., 2025. Field intercomparison of ice nucleation measurements: the fifth international workshop on ice nucleation phase 3 (FIN-03). Atmos. Meas. Tech. 18, 639–672. https://doi.org/10.5194/amt-18-639-2025.

Fan, Y., Liu, J., Shang, W., Li, J., 2025. Analysis of time- and size-resolved fluorescent biological aerosol particles in a subway station. Atmos. Environ. 350. https://doi.org/10.1016/j.atmosenv.2025.121142.

Feeney, P., Rodríguez, S.F., Molina, R., McGillicuddy, E., Hellebust, S., Quirke, M., et al., 2018. A comparison of on-line and off-line bioaerosol measurements at a biowaste site. Waste Manag. 76, 323–338. https://doi.org/10.1016/j.wasman.2018.02.035.

Fennelly, M., Sewell, G., Prentice, M., O'Connor, D., Sodeau, J., 2017. Review: the use of real-time fluorescence instrumentation to monitor ambient primary biological aerosol particles (PBAP). Atmosphere 9, 1. https://doi.org/10.3390/atmos9010001.

Fernández-Rodríguez, S., Tormo-Molina, R., Lemonis, N., Clot, B., O'Connor, D.J., Sodeau, J.R., 2018. Comparison of fungal spores concentrations measured with wideband integrated bioaerosol sensor and Hirst methodology. Atmos. Environ. 175, 1–14. https://doi.org/10.1016/j.atmosenv.2017.11.038.

Forde, E., Gallagher, M., Foot, V., Sarda-Esteve, R., Crawford, I., Kaye, P., et al., 2019a. Characterisation and source identification of biofluorescent aerosol emissions over winter and summer periods in the United Kingdom. Atmos. Chem. Phys. 19, 1665–1684. https://doi.org/10.5194/acp-19-1665-2019.

Forde, E., Gallagher, M., Walker, M., Foot, V., Attwood, A., Granger, G., et al., 2019b. Intercomparison of multiple UV-LIF spectrometers using the aerosol challenge simulator. Atmosphere 10. https://doi.org/10.3390/ATMOS10120797.

Gabey, A.M., Gallagher, M.W., Whitehead, J., Dorsey, J.R., Kaye, P.H., Stanley, W.R., 2010. Measurements and comparison of primary biological aerosol above and below a tropical forest canopy using a dual channel fluorescence spectrometer. Atmos. Chem. Phys. 10, 4453–4466. https://doi.org/10.5194/acp-10-4453-2010.

Gabey, A.M., Stanley, W.R., Gallagher, M.W., Kaye, P.H., 2011. The fluorescence properties of aerosol larger than 0.8 μ in urban and tropical rainforest locations. Atmos. Chem. Phys. 11, 5491–5504. https://doi.org/10.5194/acp-11-5491-2011.

Gabey, A.M., Vaitilingom, M., Freney, E., Boulon, J., Sellegri, K., Gallagher, M.W., et al., 2013. Observations of fluorescent and biological aerosol at a high-altitude site in central France. Atmos. Chem. Phys. 13, 7415–7428. https://doi.org/10.5194/acp-13-7415-2013.

González-Alonso, M., Oteros, J., Widmann, M., Maya-Manzano, J.M., Skjøth, C., Grewling, L., et al., 2024. Influence of meteorological variables and air pollutants on measurements from automatic pollen sampling devices. Sci. Total Environ. 931. https://doi.org/10.1016/j.scitotenv.2024.172913.

Healy, D.A., Huffman, J.A., O'Connor, D.J., Pöhlker, C., Pöschl, U., Sodeau, J.R., 2014. Ambient measurements of biological aerosol particles near Killarney, Ireland: a comparison between real-time fluorescence and microscopy techniques. Atmos. Chem. Phys. 14, 8055–8069. https://doi.org/10.5194/acp-14-8055-2014.

Healy, D.A., O'Connor, D.J., Burke, A.M., Sodeau, J.R., 2012b. A laboratory assessment of the Waveband integrated bioaerosol sensor (WIBS-4) using individual samples of pollen and fungal spore material. Atmos. Environ. 60, 534–543. https://doi.org/10.1016/j.atmosenv.2012.06.052.

Healy, D.A., O'Connor, D.J., Sodeau, J.R., 2012a. Measurement of the particle counting efficiency of the "Waveband Integrated Bioaerosol Sensor" model number 4 (WIBS-4). J. Aerosol Sci. 47, 94–99. https://doi.org/10.1016/j.jaerosci.2012.01.003.

Heim, M., Mullins, B.J., Umhauer, H., Kasper, G., 2008. Performance evaluation of three optical particle counters with an efficient "multimodal" calibration method. J. Aerosol Sci. 39, 1019–1031. https://doi.org/10.1016/j.jaerosci.2008.07.006.

Huang, Z., Yu, X., Liu, Q., Maki, T., Alam, K., Wang, Y., et al., 2024. Bioaerosols in the atmosphere: a comprehensive review on detection methods, concentration and influencing factors. Sci. Total Environ. 912, 168818. https://doi.org/10.1016/j.scitotenv.2023.168818.

Ila Gosselin, M., Rathnayake, C.M., Crawford, I., Pöhlker, C., Fröhlich-Nowoisky, J., Schmer, B., et al., 2016. Fluorescent bioaerosol particle, molecular tracer, and fungal

spore concentrations during dry and rainy periods in a semi-arid forest. Atmos. Chem. Phys. 16, 15165–15184. https://doi.org/10.5194/acp-16-15165-2016.
Lancia, A., Gioffrè, A., Di Rita, F., Magri, D., D'Ovidio, M.C., 2023. Aerobiological monitoring in an indoor occupational setting using a real-time bioaerosol sampler. Atmosphere 14. https://doi.org/10.3390/atmos14010118.
Li, J., Wan, M.P., Schiavon, S., Tham, K.W., Zuraimi, S., Xiong, J., et al., 2020. Size-resolved dynamics of indoor and outdoor fluorescent biological aerosol particles in a bedroom: a one-month case study in Singapore. Indoor Air 30, 942–954. https://doi.org/10.1111/ina.12678.
Li, J., Zuraimi, S., Schiavon, S., Wan, M.P., Xiong, J., Tham, K.W., 2022. Diurnal trends of indoor and outdoor fluorescent biological aerosol particles in a tropical urban area. Sci. Total Environ. 848. https://doi.org/10.1016/j.scitotenv.2022.157811.
Liang, L., Xu, W., Liu, C., Liu, X., Cheng, H., Liu, Y., et al., 2024. Variation characteristics of fluorescent biological aerosol particles in Beijing under springtime clean, haze and dusty condition. Urban Clim. 56. https://doi.org/10.1016/j.uclim.2024.102040.
Lieberherr, G., Auderset, K., Calpini, B., Clot, B., Crouzy, B., Gysel-Beer, M., et al., 2021. Assessment of real-time bioaerosol particle counters using reference chamber experiments. Atmos. Meas. Tech. 14, 7693–7706. https://doi.org/10.5194/amt-14-7693-2021.
Ma, Y., Wang, Z., Yang, D., Diao, Y., Wang, W., Zhang, H., et al., 2019. On-line measurement of fluorescent aerosols near an industrial zone in the Yangtze River Delta region using a wideband integrated bioaerosol spectrometer. Sci. Total Environ. 656, 447–457. https://doi.org/10.1016/j.scitotenv.2018.11.370.
Markey, E., Hourihane Clancy, J., Martínez-Bracero, M., Neeson, F., Sarda-Estève, R., Baisnée, D., et al., 2022. A modified spectroscopic approach for the real-time detection of pollen and fungal spores at a semi-urban site using the WIBS-4+, part I. Sensors 22. https://doi.org/10.3390/s22228747.
Markey, E., Hourihane Clancy, J., Martínez-Bracero, M., Sarda-Estève, R., Baisnée, D., McGillicuddy, E.J., et al., 2024. Spectroscopic detection of bioaerosols with the wibs-4+: anthropogenic and meteorological impacts. Sci. Total Environ. 943. https://doi.org/10.1016/j.scitotenv.2024.173649.
Matavulj, P., Cristofori, A., Cristofolini, F., Gottardini, E., Brdar, S., Sikoparija, B., 2022. Integration of reference data from different Rapid-E devices supports automatic pollen detection in more locations. Sci. Total Environ. 851. https://doi.org/10.1016/j.scitotenv.2022.158234.
Matavulj, P., Panić, M., Šikoparija, B., Tešendić, D., Radovanović, M., Brdar, S., 2023. Advanced CNN architectures for pollen classification: design and comprehensive evaluation. Appl. Artif. Intell. 37. https://doi.org/10.1080/08839514.2022.2157593.
Moallemi, A., Landwehr, S., Robinson, C., Simó, R., Zamanillo, M., Chen, G., et al., 2021. Sources, occurrence and characteristics of fluorescent biological aerosol particles measured over the pristine Southern Ocean. J. Geophys Res. Atmosph. 126. https://doi.org/10.1029/2021JD034811.
Morrison, D., Li, J., Crawford, I., Che, W., Flynn, M., Chan, M.N., et al., 2020. The observation and characterisation of fluorescent bioaerosols using real-time UV-LIF spectrometry in Hong Kong from June to November 2018. Atmosphere 11. https://doi.org/10.3390/atmos11090944.
Negron, A., Deleon-Rodriguez, N., Waters, S.M., Ziemba, L.D., Anderson, B., Bergin, M., et al., 2020. Using flow cytometry and light-induced fluorescence to characterize the variability and characteristics of bioaerosols in springtime in Metro Atlanta, Georgia. Atmos. Chem. Phys. 20, 1817–1838. https://doi.org/10.5194/acp-20-1817-2020.
O'Connor, D.J., Daly, S.M., Sodeau, J.R., 2015b. On-line monitoring of airborne bioaerosols released from a composting/green waste site. Waste Manag. 42, 23–30. https://doi.org/10.1016/j.wasman.2015.04.015.
O'Connor, D.J., Daly, S.M., Sodeau, J.R., 2015c. On-line monitoring of airborne bioaerosols released from a composting/green waste site. Waste Manag. 42, 23–30. https://doi.org/10.1016/j.wasman.2015.04.015.
O'Connor, D.J., Healy, D.A., Sodeau, J.R., 2013. The on-line detection of biological particle emissions from selected agricultural materials using the WIBS-4 (Waveband Integrated Bioaerosol Sensor) technique. Atmos. Environ. 80, 415–425. https://doi.org/10.1016/j.atmosenv.2013.07.051.
O'Connor, D.J., Healy, D.A., Sodeau, J.R., 2015a. A 1-month online monitoring campaign of ambient fungal spore concentrations in the harbour region of Cork, Ireland. Aerobiologia 31, 295–314. https://doi.org/10.1007/s10453-015-9365-7.
Oconnor, D.J., Healy, D.A., Hellebust, S., Buters, J.T.M., Sodeau, J.R., 2014. Using the WIBS-4 (Waveband Integrated Bioaerosol Sensor) technique for the on-line detection of pollen grains. Aerosol. Sci. Technol. 48, 341–349. https://doi.org/10.1080/02786826.2013.872768.
Page, M.J., McKenzie, J.E., Bossuyt, P.M., Boutron, I., Hoffmann, T.C., Mulrow, C.D., et al., 2021. The PRISMA 2020 statement: an updated guideline for reporting systematic reviews. Int. J. Surg. 88, 105906. https://doi.org/10.1016/j.ijsu.2021.105906.
Perring, A.E., Mediavilla, B., Wilbanks, G.D., Churnside, J.H., Marchbanks, R., Lamb, K. D., et al., 2023. Airborne bioaerosol observations imply a strong terrestrial source in the summertime arctic. J. Geophys Res. Atmosph. 128. https://doi.org/10.1029/2023JD039165.
Perring, A.E., Schwarz, J.P., Baumgardner, D., Hernandez, M.T., Spracklen, D.V., Heald, C.L., et al., 2015. Airborne observations of regional variation in fluorescent aerosol across the United States. J. Geophys. Res. 120, 1153–1170. https://doi.org/10.1002/2014JD022495.
Pöhlker, C., Huffman, J.A., Pöschl, U., 2012. Autofluorescence of atmospheric bioaerosols – fluorescent biomolecules and potential interferences. Atmos. Meas. Tech. 5, 37–71. https://doi.org/10.5194/amt-5-37-2012.
Robinson, E.S., Gao, R.-S., Schwarz, J.P., Fahey, D.W., Perring, A.E., 2017. Fluorescence calibration method for single-particle aerosol fluorescence instruments. Atmos. Meas. Tech. 10, 1755–1768. https://doi.org/10.5194/amt-10-1755-2017.
Robinson, N.H., Allan, J.D., Huffman, J.A., Kaye, P.H., Foot, V.E., Gallagher, M., 2013. Cluster analysis of WIBS single-particle bioaerosol data. Atmos. Meas. Tech. 6, 337–347. https://doi.org/10.5194/amt-6-337-2013.
Ruske, S., Topping, D.O., Foot, V.E., Morse, A.P., Gallagher, M.W., 2018. Machine learning for improved data analysis of biological aerosol using the WIBS. Atmos. Meas. Tech. 11, 6203–6230. https://doi.org/10.5194/amt-11-6203-2018.
Santander, M.V., Mitts, B.A., Pendergraft, M.A., Dinasquet, J., Lee, C., Moore, A.N., et al., 2021. Tandem fluorescence measurements of organic matter and bacteria released in sea spray aerosols. Environ. Sci. Technol. 55, 5171–5179. https://doi.org/10.1021/acs.est.0c05493.
Sarangi, B., Baumgardner, D., Bolaños-Rosero, B., Mayol-Bracero, O.L., 2022. Measurement report: an exploratory study of fluorescence and cloud condensation nuclei activity of urban aerosols in San Juan, Puerto Rico. Atmos. Chem. Phys. 22, 9647–9661. https://doi.org/10.5194/acp-22-9647-2022.
Sarangi, B., Baumgardner, D., Calvo, A.I., Bolaños-Rosero, B., Fraile, R., Rodríguez-Fernández, A., et al., 2025. Measurement report: a comparative analysis of an intensive incursion of fluorescing African dust particles over Puerto Rico and another over Spain. Atmos. Chem. Phys. 25, 843–865. https://doi.org/10.5194/acp-25-843-2025.
Savage, N.J., Krentz, C.E., Könemann, T., Han, T.T., Mainelis, G., Pöhlker, C., et al., 2017. Systematic characterization and fluorescence threshold strategies for the wideband integrated bioaerosol sensor (WIBS) using size-resolved biological and interfering particles. Atmos. Meas. Tech. 10, 4279–4302. https://doi.org/10.5194/amt-10-4279-2017.
Savage, N.J., Huffman, J.A., 2018. Evaluation of a hierarchical agglomerative clustering method applied to WIBS laboratory data for improved discrimination of biological particles by comparing data preparation techniques. Atmos. Meas. Tech. 11, 4929–4942. https://doi.org/10.5194/amt-11-4929-2018.
Shawon, A.S.M., Benedict, K.B., Gutierrez, A., Aiken, A.C., 2025. Diurnal trends and meteorological factors influencing the variability of fluorescent bioaerosol in Mt. Crested butte, Colorado during SAIL. J. Geophys Res. Atmosph. 130. https://doi.org/10.1029/2024JD041186.
Sikoparija, B., Matavulj, P., Simovic, I., Radisic, P., Brdar, S., Minic, V., et al., 2024. Classification accuracy and compatibility across devices of a new Rapid-E+ flow cytometer. Atmos. Meas. Tech. 17, 5051–5070. https://doi.org/10.5194/amt-17-5051-2024.
Smith, M., Matavulj, P., Mimić, G., Panić, M., Grewling, Ł., Šikoparija, B., 2022. Why should we care about high temporal resolution monitoring of bioaerosols in ambient air? Sci. Total Environ. 826. https://doi.org/10.1016/j.scitotenv.2022.154231.
Tang, D., Wei, T., Yuan, J., Xia, H., Dou, X., 2022. Observation of bioaerosol transport using wideband integrated bioaerosol sensor and coherent Doppler lidar. Atmos. Meas. Tech. 15, 2819–2838. https://doi.org/10.5194/amt-15-2819-2022.
Tešendić, D., Boberić Krstićev, D., Matavulj, P., Brdar, S., Panić, M., Minić, V., et al., 2020. RealForAll: real-time system for automatic detection of airborne pollen. Enterp. Inf. Syst. 1–17. https://doi.org/10.1080/17517575.2020.1793391.
Toprak, E., Schnaiter, M., 2013a. Fluorescent biological aerosol particles measured with the waveband integrated bioaerosol sensor WIBS-4: laboratory tests combined with a one year field study. Atmos. Chem. Phys. 13, 225–243. https://doi.org/10.5194/acp-13-225-2013.
Toprak, E., Schnaiter, M., 2013b. Fluorescent biological aerosol particles measured with the Waveband integrated bioaerosol sensor WIBS-4: laboratory tests combined with a one year field study. Atmos. Chem. Phys. 13, 225–243. https://doi.org/10.5194/acp-13-225-2013.
Tummon, F., Adamov, S., Clot, B., Crouzy, B., Gysel-Beer, M., Kawashima, S., et al., 2024. A first evaluation of multiple automatic pollen monitors run in parallel. Aerobiologia 40, 93–108. https://doi.org/10.1007/s10453-021-09729-0.
Venkatesan, S., Zare, A., Ristovski, Z.D., Niazi, S., Vahaji, S., Lampugnani, E.R., et al., 2025. Simulation of pollen–humidity interactions and origin of airborne sub-pollen particles. Sci. Total Environ. 966. https://doi.org/10.1016/j.scitotenv.2025.178706.
Wei, Y., Yu, Y., Cao, X., Wang, B., Yu, D., Wang, J., et al., 2024. Remote mountainous area inevitably becomes temporal sink for microplastics driven by atmospheric transport. Environ. Sci. Technol. https://doi.org/10.1021/acs.est.4c00296 acs.est.4c00296.
Whitehead, J.D., Darbyshire, E., Brito, J., Barbosa, H.M.J., Crawford, I., Stern, R., et al., 2016. Biogenic cloud nuclei in the central Amazon during the transition from wet to dry season. Atmos. Chem. Phys. 16, 9727–9743. https://doi.org/10.5194/acp-16-9727-2016.
Whitehead, J.D., Gallagher, M.W., Dorsey, J.R., Robinson, N., Gabey, A.M., Coe, H., et al., 2010. Aerosol fluxes and dynamics within and above a tropical rainforest in South-East Asia. Atmos. Chem. Phys. 10, 9369–9382. https://doi.org/10.5194/acp-10-9369-2010.
Wingert, L., Debia, M., Hallé, S., Marchand, G., 2022. Occupational microbial risk among embalmers. Atmosphere 13. https://doi.org/10.3390/atmos13081281.
Xie, Y., Fajardo, O.A., Yan, W., Zhao, B., Jiang, J., 2017. Six-day measurement of size-resolved indoor fluorescent bioaerosols of outdoor origin in an office. Particuology 31, 161–169. https://doi.org/10.1016/j.partic.2016.09.004.
Xie, Y., Wang, Y., He, J., Yang, X., Duan, X., Zhao, B., 2024. Human emissions of size-resolved fluorescent bioaerosols in control situations. Sci. Total Environ. 926. https://doi.org/10.1016/j.scitotenv.2024.171661.
Yu, X., Wang, Z., Zhang, M., Kuhn, U., Xie, Z., Cheng, Y., et al., 2016. Ambient measurement of fluorescent aerosol particles with a WIBS in the Yangtze River Delta of China: potential impacts of combustion-related aerosol particles. Atmos. Chem. Phys. 16, 11337–11348. https://doi.org/10.5194/acp-16-11337-2016.
Yue, S., Li, L., Xu, W., Zhao, J., Ren, H., Ji, D., et al., 2022. Biological and nonbiological sources of fluorescent aerosol particles in the urban atmosphere. Environ. Sci. Technol. 56, 7588–7597. https://doi.org/10.1021/acs.est.1c07966.

Yue, S., Ren, H., Fan, S., Wei, L., Zhao, J., Bao, M., et al., 2017. High abundance of Fluorescent biological aerosol particles in winter in Beijing, China. ACS Earth Space Chem. 1, 493–502. https://doi.org/10.1021/acsearthspacechem.7b00062.

Yue, S., Ren, L., Song, T., Li, L., Xie, Q., Li, W., et al., 2019. Abundance and diurnal trends of fluorescent bioaerosols in the troposphere over Mt. Tai, China, in spring. J. Geophys Res. Atmosph. 124, 4158–4173. https://doi.org/10.1029/2018JD029486.

Zhang, H.H., Lai, A.C.K., 2025. Characteristic of real-time airborne bacteria measurement and the response of low-cost particulate matter sensor: a pilot study. J. Build. Eng. 110. https://doi.org/10.1016/j.jobe.2025.113021.

Zhou, J., Fang, W., Cao, Q., Yang, L., Chang, V.W.-C., Nazaroff, W.W., 2017. Influence of moisturizer and relative humidity on human emissions of fluorescent biological aerosol particles. Indoor Air 27, 587–598. https://doi.org/10.1111/ina.12349.